WIND TUNNEL TESTS ON THE EFFECT OF POWER ON THE STABILITY OF A LOW WING MONOPLANE WITH THREE VERTICAL POSITIONS OF HORIZONTAL TAIL SURFACES

Thesis by

Calvin M. Bolster

In partial fulfillment of the requirements for

the Degree of Master of Science in Aeronautical Engineering

California Institute of Technology
Pasadena, California
1936

TABLE OF NOTATIONS

a = slipstream factor, explained in text.

a_o = $\frac{dC_L}{d\alpha_o}$ = slope of lift curve for infinite aspect ratio.

AR = aspect ratio of wing.

AR_t = aspect ratio of tail surfaces.

b = wing span.

b_e = portion of span effected by slipstream.

b_t = horizontal tail surface span.

b_{t_e} = span of tail surfaces in slipstream.

C_D = drag coefficient = $\frac{D}{qS}$.

C_{D_r} = resultant drag coefficient = $\frac{D-T}{qS}$.

C.G. = center of gravity of airplane.

C_L = lift coefficient = $\frac{L}{qS}$.

C_M = pitching moment coefficient = $\frac{M}{qSt}$

C_{M_o} = moment coefficient of wing about mean aerodynamic center

C_{M_W} = pitching moment coefficient of wing alone.

$C_{M_{W+F}}$ = pitching moment coefficient of wing and fuselage = C_M no tail.

C_{M_t} = pitching moment coefficient of tail.

$C_{M_{th}}$ = pitching moment coefficient due to thrust.

C_T' = thrust coefficient used in slipstream calculations = $\frac{T}{q\frac{\pi D_o^2}{4}}$

C_{M_F} = pitching moment coefficient of fuselage

d = distance from leading edge of wing to C. G.

D = drag, a force parallel to air velocity.

D_P = propeller diameter.

D_o = theoretical slipstream diameter.

D_S = calculated diameter of slipstream around fuselage.

K = a factor as explained in text.

L = lift, a force normal to air velocity.

l = tail length, C.G. to elevator hinge.

M = pitching moment of model about C. G.

M_e = pitching moment over portion of wing in slipstream.

M_r = pitching moment over portion of wing not in slipstream.

q = dynamic pressure = $\frac{1}{2}\rho v^2$.

qS = dynamic pressure in slipstream = $\frac{1}{2}\rho v_S^2$.

R = a factor as explained in text.

S = wing area.

S_e = wing area effected by slipstream.

S_t = tail area (horizontal surfaces).

t = mean aerodynamic chord length.

v = air velocity.

V_S = slipstream velocity.

W = weight of airplane.

α = angle of attack.

α_d = aerodynamic decalage.

Δ = "increment of".

η_t = tail efficiency.

θ = angle of climb or glide.

ρ = air density.

$()'$ = $()$ "power on," e. g. $C_L' = C_L$ "power on," etc.

h = distance from leading edge of wing to mean aerodynamic center

ΔC_{M_o} = increment of moment coefficient change at $C_L = 0$ due to fuselage

LIST OF ILLUSTRATIONS AND CHARTS

WIND TUNNEL TESTS ON THE EFFECT OF POWER ON THE STABILITY OF A LOW WING MONOPLANE WITH THREE VERTICAL POSITIONS OF HORIZONTAL TAIL SURFACES

INTRODUCTION

A great majority of present day airplanes are of the low wing cantilever type. An investigation into the effect of power and vertical location of the horizontal tail surfaces on the longitudinal static stability of such airplanes is therefore of interest.

The present investigation was carried out on a one-sixth scale model of a low wing single engine tractor monoplane. The results are probably most directly applicable to airplanes of this type. However, the tendencies and general effects should also be fairly indicative of what may be expected in multiple engine low wing monoplanes of conventional design.

A composite model was used consisting of a Northrop "Alpha" wing and fuselage and XTBD - 1 tail surfaces. This model is the same as the one used by J. S. Russell and H. M. McCoy, in their investigation "Wind Tunnel Tests on a High Wing Monoplane with Running Propeller", reported in the Journal of Aeronautical Sciences dated January, 1936, except that different tail surfaces were used, a different torque measuring mechanism was used, and for this investigation it was converted into a low wing monoplane. An N.A.C.A. cowling with air-cooled engine was used and the model was complete except for landing gear, tail wheel and protruding cockpit enclosures. A conventional fillet between fuselage and upper surface of wing was developed. This fillet was used on all tests. Figure 5 gives the principal characteristics and dimensions of the model.

The propeller used was a three bladed fixed pitch metal propeller eighteen inches in diameter, each blade of which was one-sixth full scale in all linear dimensions. The Hamilton Standard 1A1-0 blade form was used, except that one inch, or 10 per cent, of the radius was cut off at the tip of each blade, blades being set at 29° at three-quarters radius. Power was approximately 1/36 full scale power and propeller revolutions were six times full scale revolutions. Linear velocities of propeller blade elements equaled full scale velocities. Hence, slip stream effects should closely simulate full scale effects.

DESCRIPTION OF APPARATUS

The investigation was conducted in the G.A.L.C.I.T. wind tunnel, the six component balance system shown in Figure 1 being used to measure net thrust or drag, lift and pitching moment. Geometrical angle of attack is accurately set and wind tunnel velocity is controlled within narrow limits.

Torque of the propeller motor in the model was measured by an alternating current wheatstone bridge. Torque developed by the propeller reacts on the motor stator. Rotation of the stator is opposed by a tension spring as shown in Figure 2, and the angular movement of the stator is thus a measure of the torque. This displacement moves a soft iron armature placed between two coils and varies the impedance of the circuit, thus indicating torque when properly calibrated. Propeller revolutions are measured by a counting system, shown in Figure 3. This consists of a pendulum actuated, multiple relay circuit which counts the motor revolutions over an accurate time interval of ten seconds.

The photographs, Figure 4, show the model in the various configurations tested.

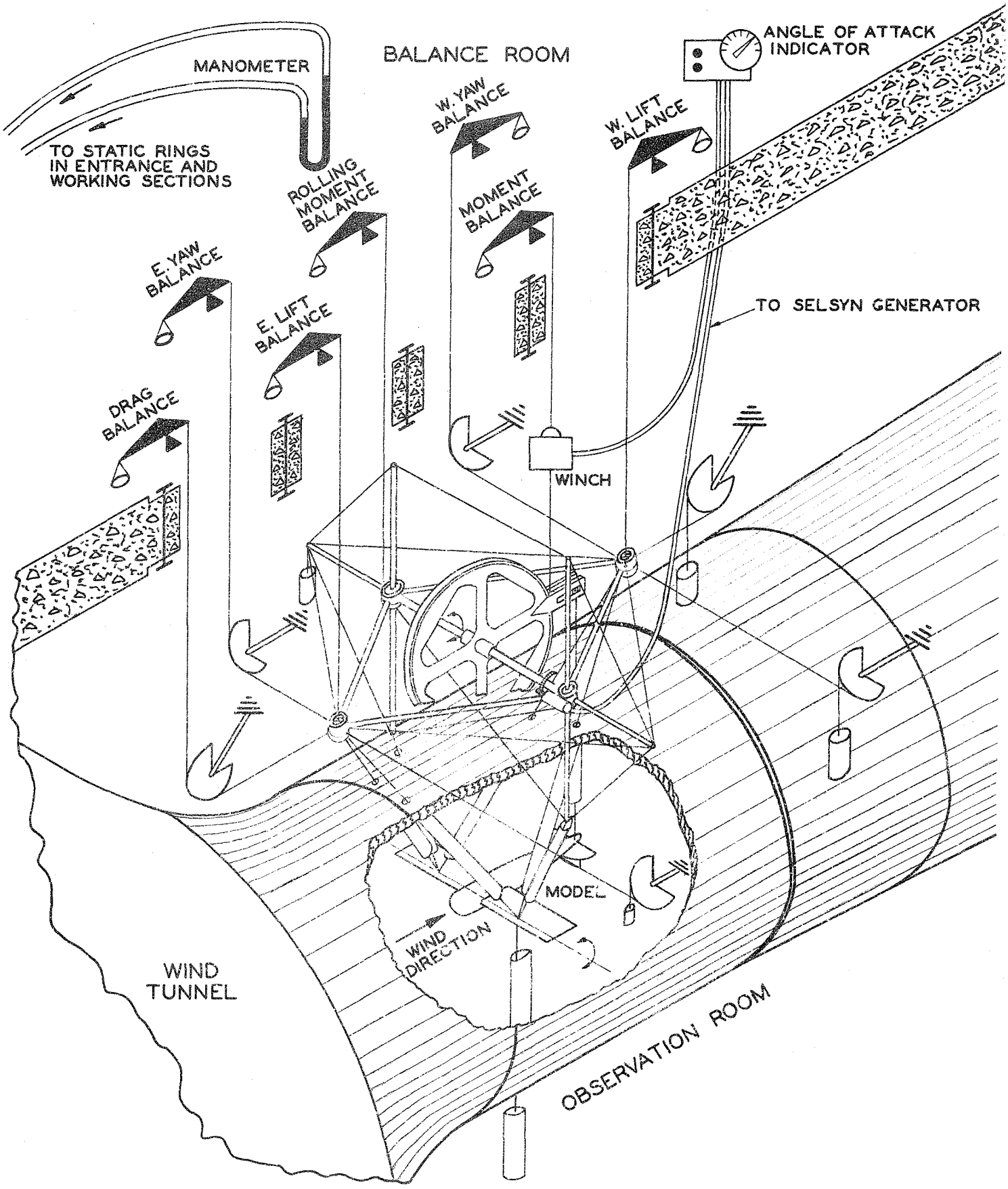

SIX COMPONENT SETUP FOR TEN FOOT WIND TUNNEL TESTS
AT GUGGENHEIM AERONAUTICS LABORATORY
CALIFORNIA INSTITUTE OF TECHNOLOGY

FIG. 1

DWG WT 26

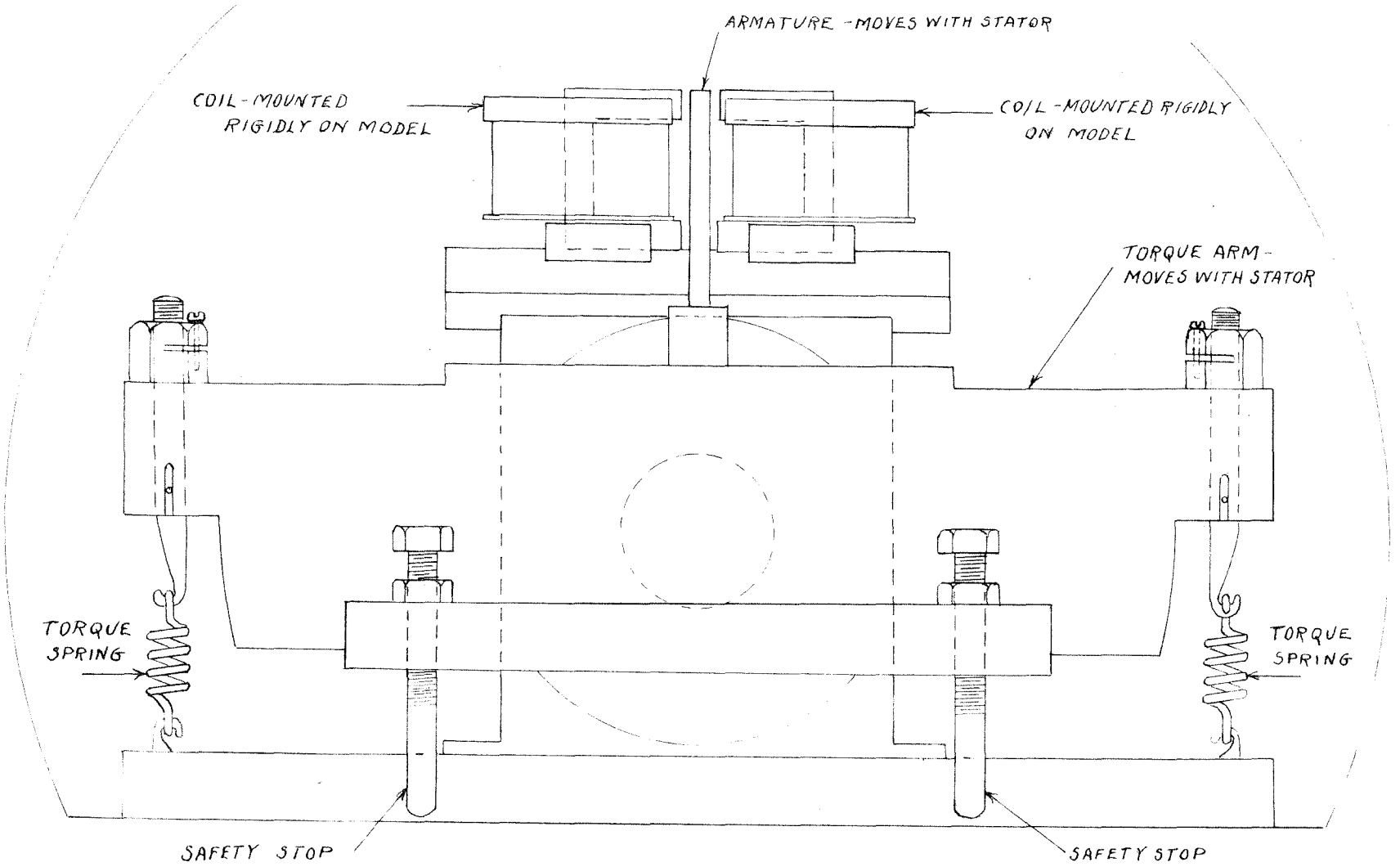

VIEW INSIDE MODEL LOOKING FORWARD
OF
TORQUE MECHANISM IN POWER MODEL

FIG. 2

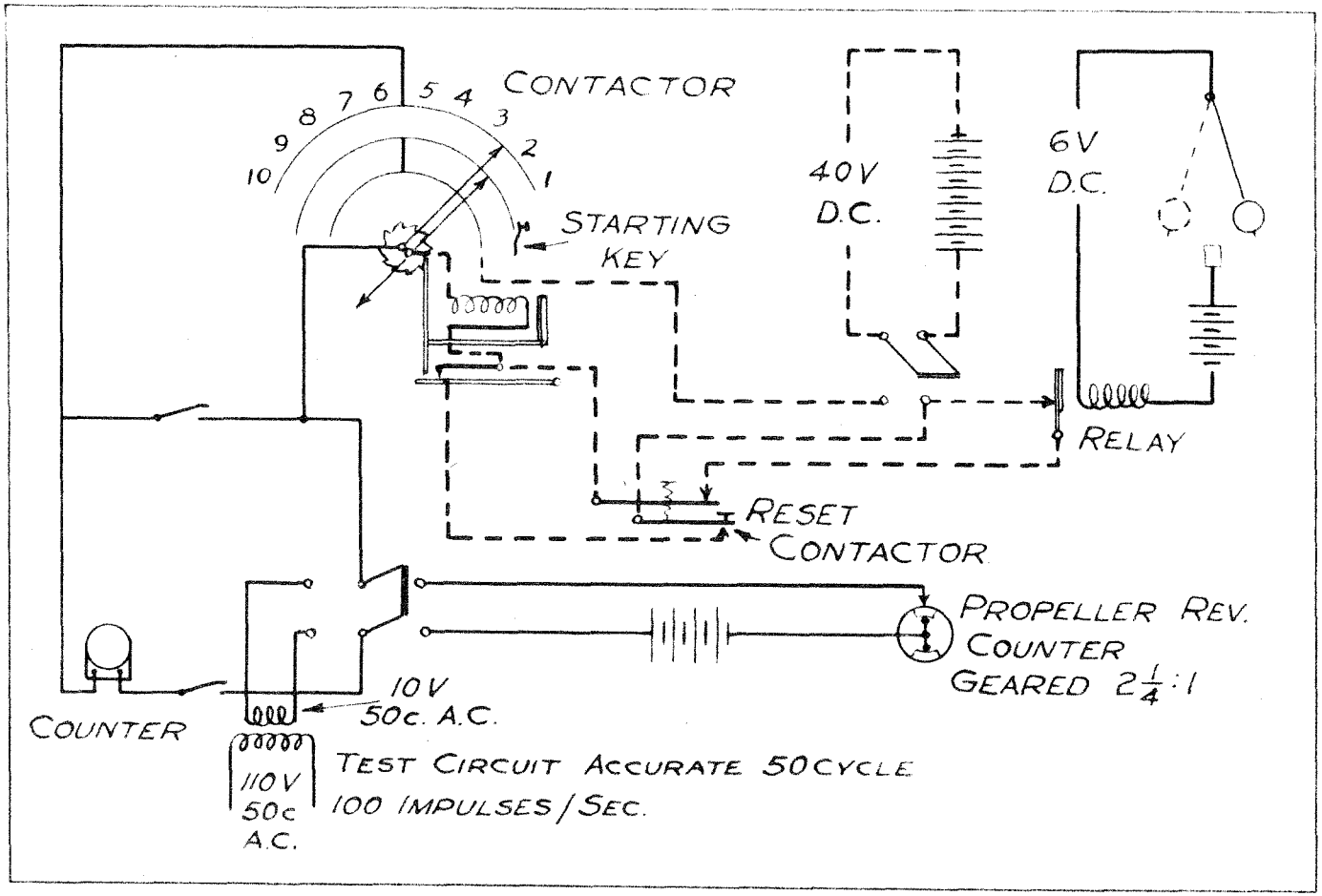
CONTACTOR
10
9
8
7
6
5
4
3
2
1
STARTING KEY
40V D.C.
6V D.C.
RELAY
RESET CONTACTOR
PROPELLER REV. COUNTER GEARED 2 1/4 : 1
10V 50c. A.C.
COUNTER
110V 50c A.C.
TEST CIRCUIT ACCURATE 50CYCLE
100 IMPULSES/SEC.

FIG. 3

VIEWS OF MODEL USED IN INVESTIGATION

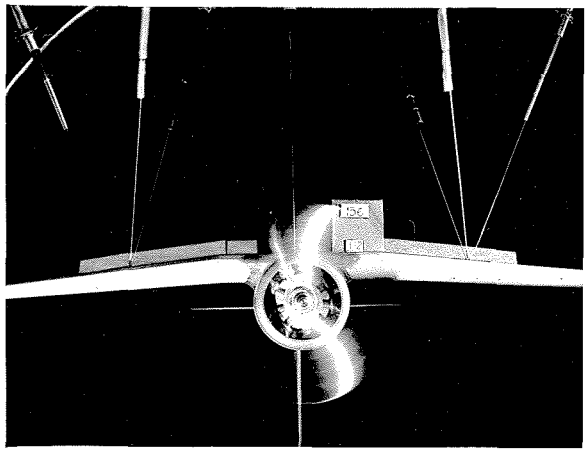

STABILIZER IN BOTTOM POSITION
WITH FLAPS CUT OUT UNDER FUSELAGE

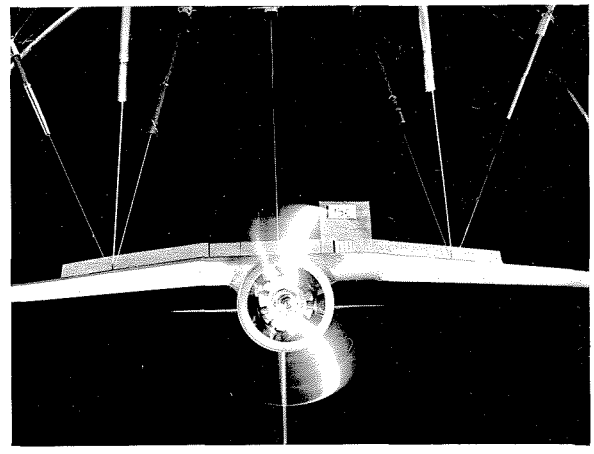

STABILIZER IN BOTTOM POSITION
WITH FLAPS CONTINUOUS UNDER FUSELAGE

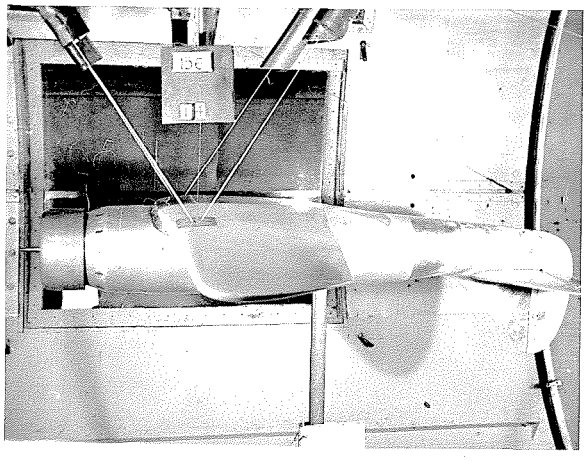

STABILIZER IN UPPER MIDDLE
POSITION

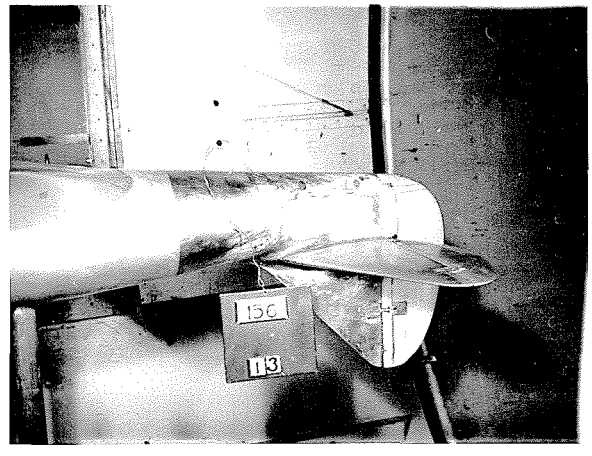

STABILIZER IN UPPER MIDDLE
POSITION

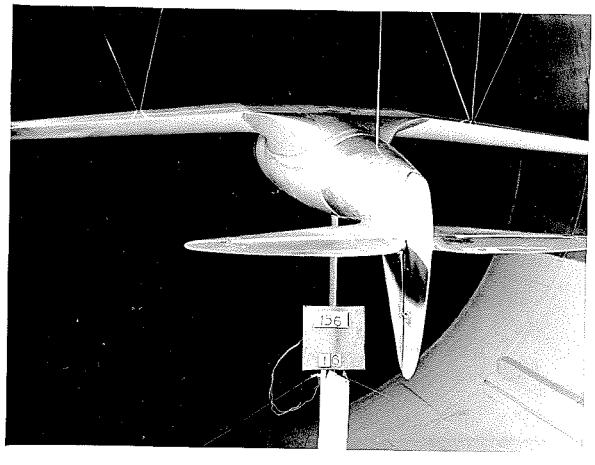

STABILIZER IN TOP POSITION
REAR VIEW

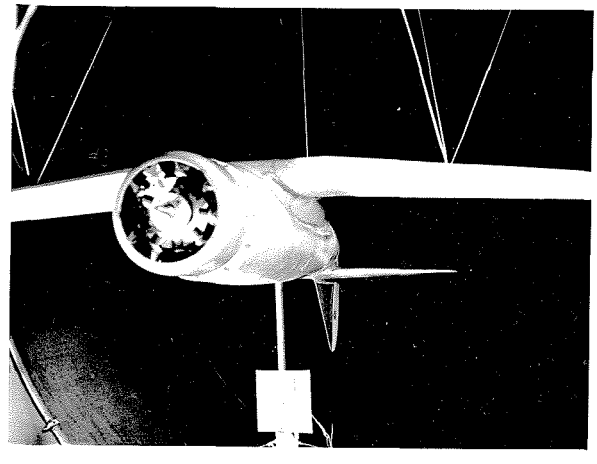

STABILIZER IN TOP POSITION
FRONT VIEW

FIG. 4

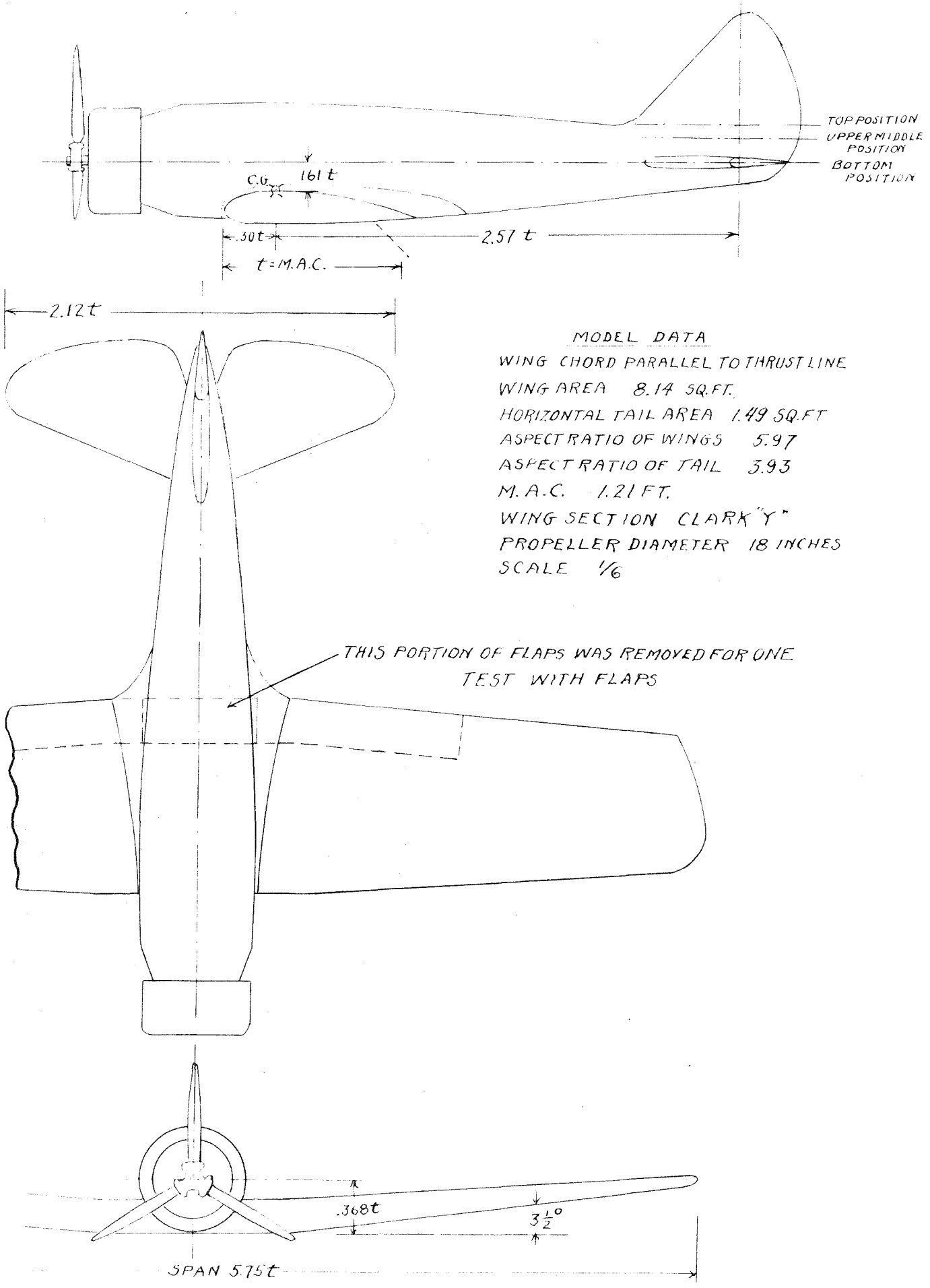
TOP POSITION
UPPER MIDDLE POSITION
BOTTOM POSITION
C.G.
.161 t
.30t
2.57 t
t = M.A.C.
2.12t
MODEL DATA
WING CHORD PARALLEL TO THRUST LINE
WING AREA 8.14 SQ.FT.
HORIZONTAL TAIL AREA 1.49 SQ.FT.
ASPECT RATIO OF WINGS 5.97
ASPECT RATIO OF TAIL 3.93
M.A.C. 1.21 FT.
WING SECTION CLARK "Y"
PROPELLER DIAMETER 18 INCHES
SCALE 1/6
THIS PORTION OF FLAPS WAS REMOVED FOR ONE TEST WITH FLAPS
.368t
3 1/2°
SPAN 5.75t

FIG. 5

PROCEDURE

In order to investigate the effect of power on the stability of this airplane under various flight conditions, it was necessary to use varying amounts of power at each air speed (wind tunnel q) and at each angle of attack. The power input was controlled by adjusting the torque, and revolutions of the propeller. At each velocity and angle of attack the revolutions of propeller and torque were varied through from four to six points in such a way that the complete flying range was covered, from less than power required for horizontal flight to more than maximum power available in a comparable airplane. In plotting results this power variation is shown as a variation in the angle of climb or glide.

Values of pitching moment coefficient, lift coefficient and resultant drag coefficient at various angles of attack were determined for the complete airplane model without propeller and with the propeller running, using varying amounts of power and with elevator neutral, down 17°, up 15° and up 25°. This was done for the following configurations:

a) Wing and fuselage with no tail surfaces.

b) Complete airplane with horizontal stabilizer in bottom position (on thrust line).

c) Complete airplane with horizontal stabilizer in upper middle position (2 inches or .14 x M.A.C. above thrust line).

d) Complete airplane with horizontal stabilizer in top position (3 inches or .21 x M.A.C. above thrust line).

e) Complete airplane with horizontal stabilizer in bottom position with split flaps set at 45 degrees extending one-half the span and continuous under the fuselage.

f) Complete airplane with horizontal stabilizer in bottom position with split flaps set at 45 degrees extending one-half the span and cut out under the fuselage.

The data for power off were plotted and curves of C_M versus C_L drawn in the conventional manner.

Each point in the "power on" data corresponds to a definite amount of power. For each such point, the value of the tangent of the angle of climb ($-C_{R/C_L}$) was calculated and recorded opposite the point. With all such points plotted it is possible to interpolate and locate points of $\tan \theta = 0$ (level flight); $\tan \theta = -.05$, $-.10$ or $-.15$ (gliding flight) or $\tan \theta = +.05$, $+.10$ (climbing flight). Curves of C_M vs. C_L for varying amounts of power (tangent θ) were then drawn in.

The curves of moment coefficient versus lift coefficient with no propeller and with power on, for wing and fuselage with no tail surfaces, were drawn in the same manner. In order to obtain tail moment coefficients, values of moment coefficient for complete airplane and for wing and fuselage alone were tabulated and tail moment coefficients found by subtraction. These values were plotted and straight lines faired through them in the region below the stall. The slopes and intercepts of these faired straight lines, shown in Figure 12, were used in calculating the tail moment factors given in Figures 13 and 14.

ANALYSIS OF RESULTS

(a) Method of Presentation

A brief description is necessary in order to clarify the method of presenting results. Consider an airplane traveling along a flight path parallel to the thrust line in unaccelerated flight:

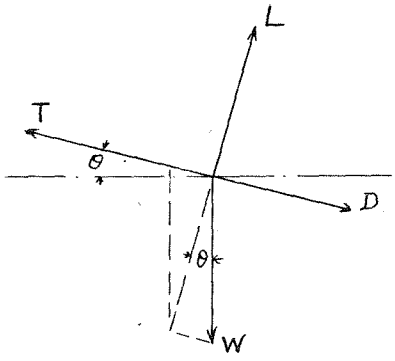

If T = thrust

D = drag

θ = angle of climb

W = weight

Then $T = D + W \sin\theta$

$T - D$ = net thrust $= W \sin\theta$

$L = W \cos\theta$

$$\frac{T - D}{L} = -\frac{C_R}{C_L} = \frac{W \sin\theta}{W \cos\theta} = \tan\theta$$

The tangent of θ, the angle of climb or glide is a measure of the amount of thrust being developed by the propeller. It is thus a convenient power parameter for wind tunnel tests since C_R and C_L may be calculated directly from the wind tunnel data. "Power on" results are given in terms of C_M vs. C_L for various values of the tangent of the angle of climb or glide.

(b) Complete Airplane

The effect of power on the static longitudinal stability of the complete airplane does not lend itself to analysis until broken down into wing and fuselage effects and tail effects. However, it is interesting to note the variation in results obtained with this model where only the vertical height of the horizontal stabilizer was changed. As the vertical position was varied, the stabilizer setting was altered in such a way that the airplane

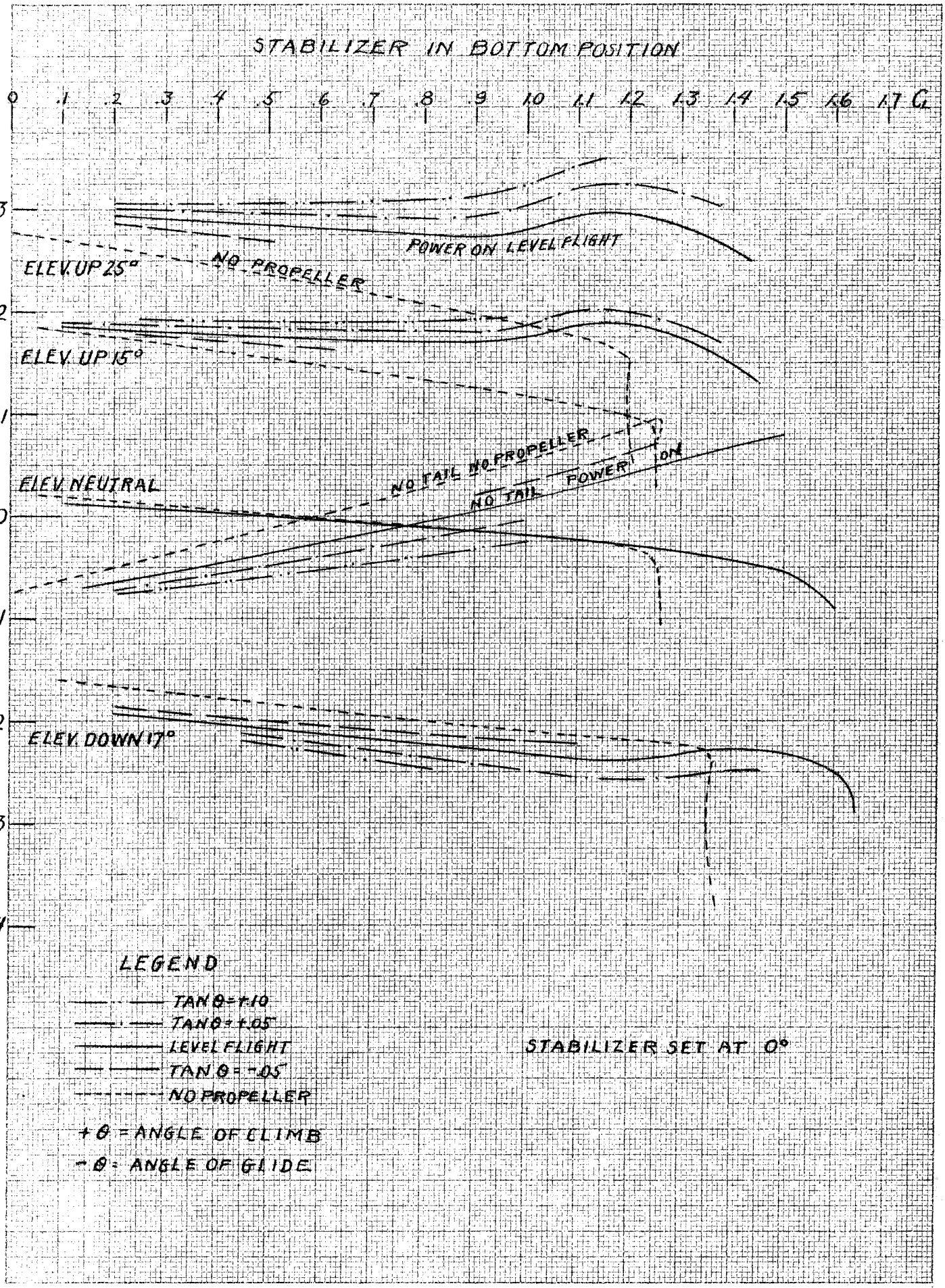
STABILIZER IN BOTTOM POSITION
0 .1 .2 .3 .4 .5 .6 .7 .8 .9 1.0 1.1 1.2 1.3 1.4 1.5 1.6 1.7 C_L
.3
.2
.1
0
-.1
-.2
-.3
-.4
C_M
POWER ON LEVEL FLIGHT
ELEV. UP 25°
NO PROPELLER
ELEV. UP 15°
NO TAIL NO PROPELLER
NO TAIL POWER ON
ELEV. NEUTRAL
ELEV. DOWN 17°
LEGEND
TAN θ = +.10
TAN θ = +.05
LEVEL FLIGHT
TAN θ = -.05
NO PROPELLER
+θ = ANGLE OF CLIMB
-θ = ANGLE OF GLIDE
STABILIZER SET AT 0°

FIG. 6

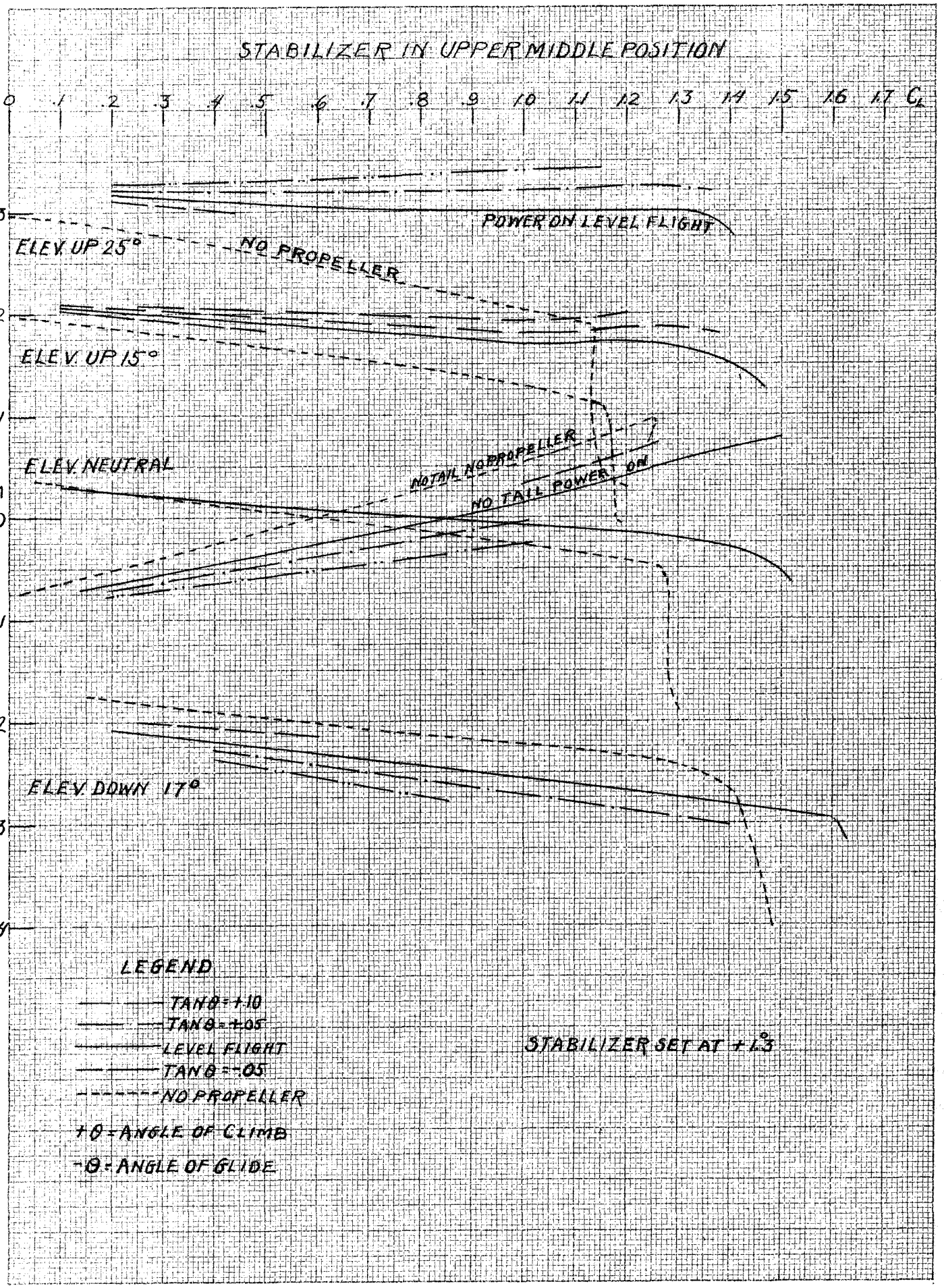
STABILIZER IN UPPER MIDDLE POSITION
0 .1 .2 .3 .4 .5 .6 .7 .8 .9 1.0 1.1 1.2 1.3 1.4 1.5 1.6 1.7 C_L
.3
.2
.1
0
-.1
-.2
-.3
-.4
C_M
POWER ON LEVEL FLIGHT
ELEV. UP 25°
NO PROPELLER
ELEV. UP 15°
ELEV. NEUTRAL
NO TAIL NO PROPELLER
NO TAIL POWER ON
ELEV. DOWN 17°
LEGEND
TAN θ = +.10
TAN θ = +.05
LEVEL FLIGHT
TAN θ = -.05
NO PROPELLER
+θ = ANGLE OF CLIMB
-θ = ANGLE OF GLIDE
STABILIZER SET AT +1.3°

FIG. 7

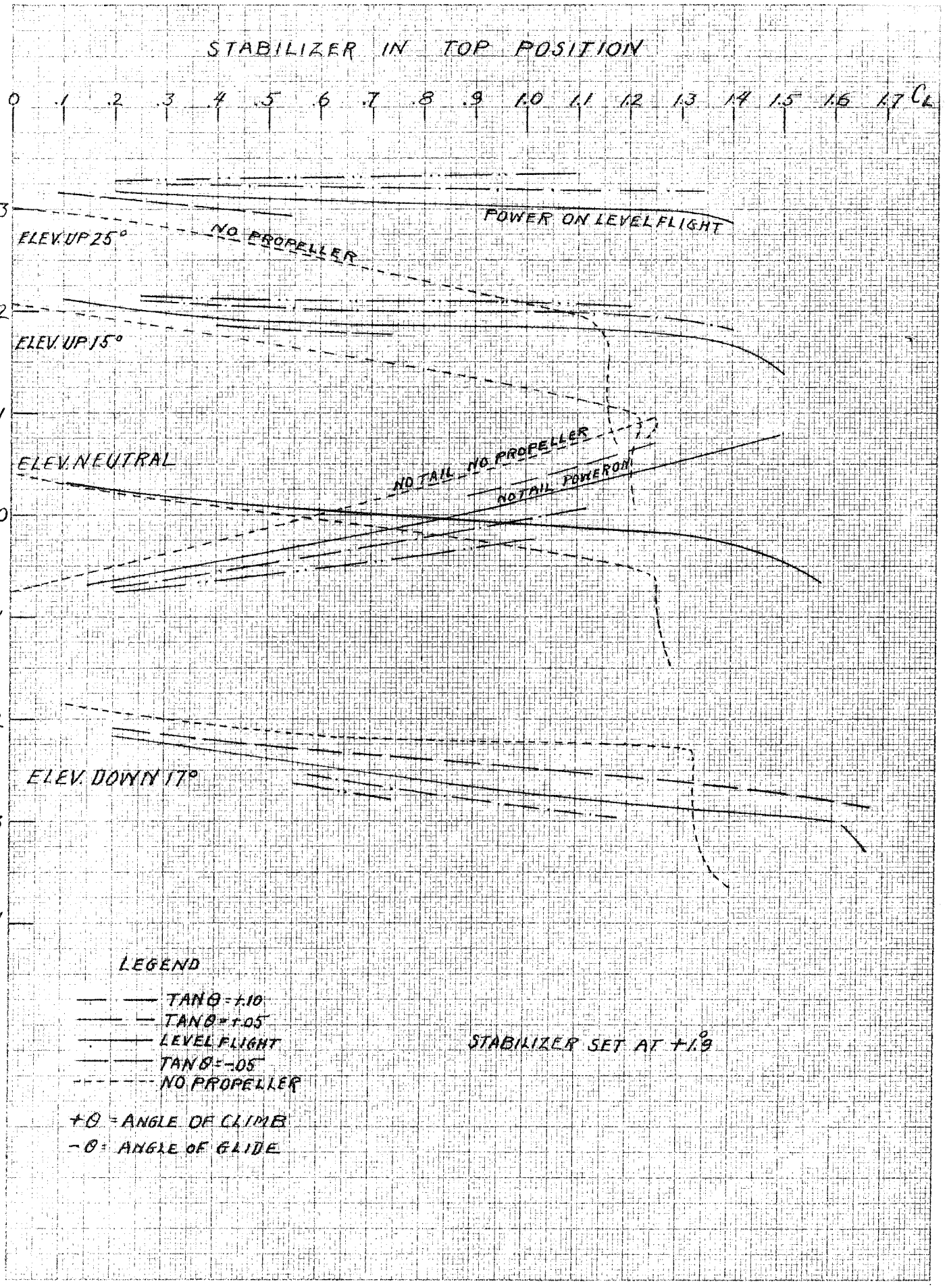
STABILIZER IN TOP POSITION
0 .1 .2 .3 .4 .5 .6 .7 .8 .9 1.0 1.1 1.2 1.3 1.4 1.5 1.6 1.7 C_L
.3
.2
.1
0
-.1
-.2
-.3
-.4
C_M
POWER ON LEVEL FLIGHT
ELEV. UP 25°
NO PROPELLER
ELEV. UP 15°
ELEV. NEUTRAL
NO TAIL NO PROPELLER
NO TAIL POWER ON
ELEV. DOWN 17°
LEGEND
TAN θ = +.10
TAN θ = +.05
LEVEL FLIGHT
TAN θ = -.05
NO PROPELLER
+θ = ANGLE OF CLIMB
-θ = ANGLE OF GLIDE
STABILIZER SET AT +1.9°

FIG. 8

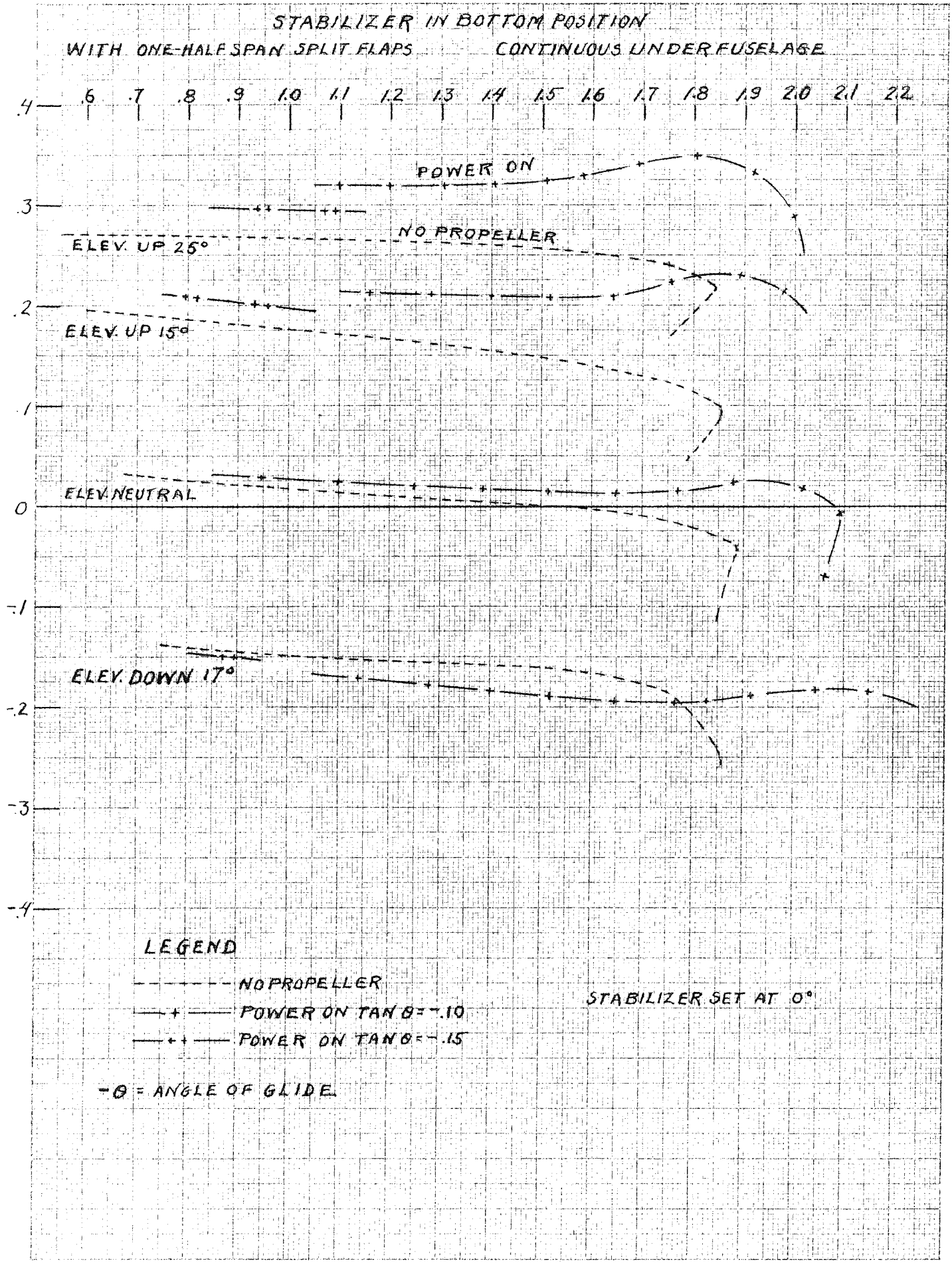
STABILIZER IN BOTTOM POSITION
WITH ONE-HALF SPAN SPLIT FLAPS CONTINUOUS UNDER FUSELAGE
.6 .7 .8 .9 1.0 1.1 1.2 1.3 1.4 1.5 1.6 1.7 1.8 1.9 2.0 2.1 2.2
.4
.3
.2
.1
0
-.1
-.2
-.3
-.4
POWER ON
NO PROPELLER
ELEV. UP 25°
ELEV. UP 15°
ELEV. NEUTRAL
ELEV. DOWN 17°
LEGEND
NO PROPELLER
POWER ON TAN θ = -.10
POWER ON TAN θ = -.15
-θ = ANGLE OF GLIDE
STABILIZER SET AT 0°

FIG. 9

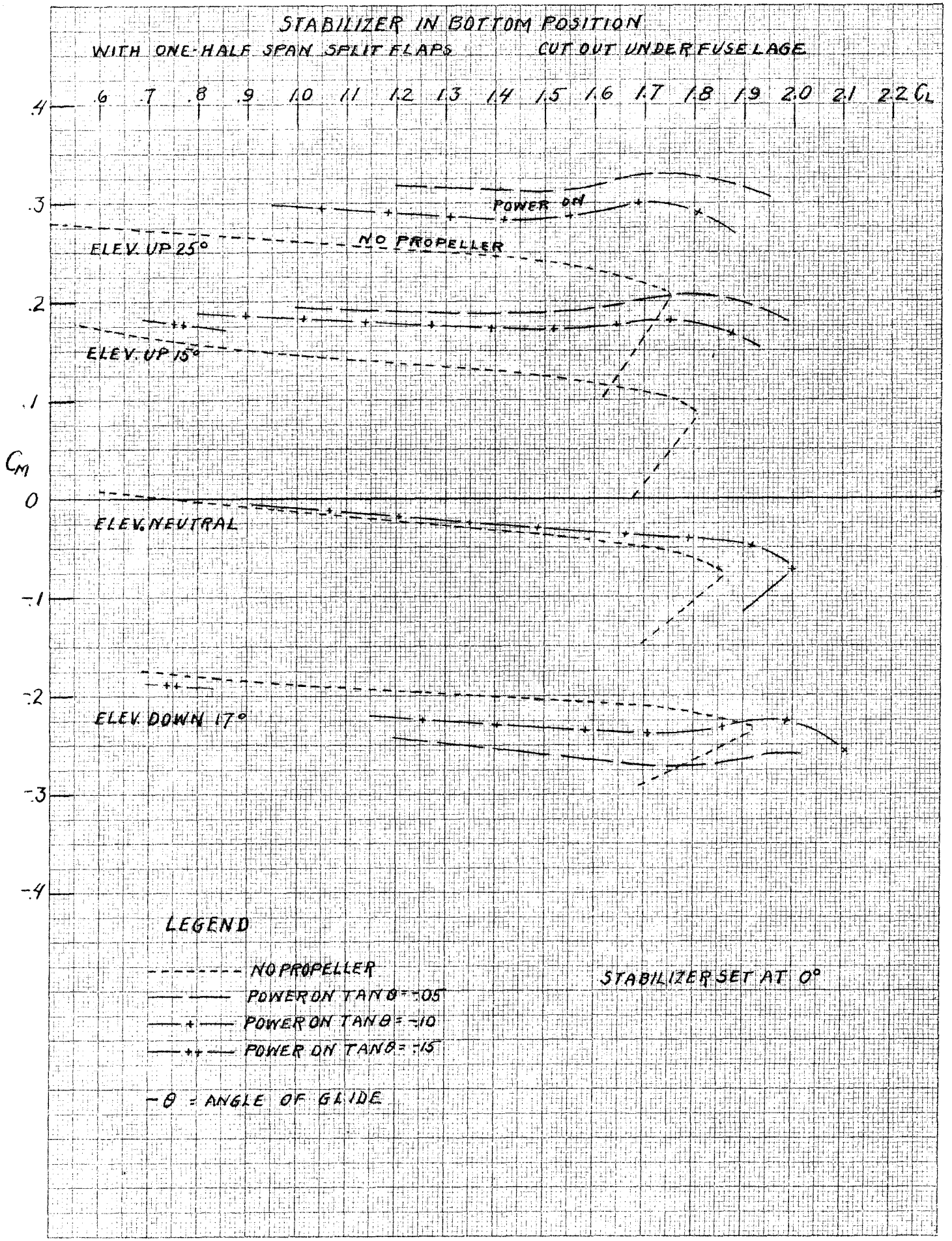
STABILIZER IN BOTTOM POSITION
WITH ONE-HALF SPAN SPLIT FLAPS CUT OUT UNDER FUSELAGE
.6 .7 .8 .9 1.0 1.1 1.2 1.3 1.4 1.5 1.6 1.7 1.8 1.9 2.0 2.1 2.2 C_L
.4
.3
.2
.1
0
-.1
-.2
-.3
-.4
C_M
POWER ON
NO PROPELLER
ELEV. UP 25°
ELEV. UP 15°
ELEV. NEUTRAL
ELEV. DOWN 17°
LEGEND
NO PROPELLER
POWER ON TAN θ = .05
POWER ON TAN θ = .10
POWER ON TAN θ = .15
θ = ANGLE OF GLIDE
STABILIZER SET AT 0°

FIG. 10

trimmed at approximately the same lift coefficient in all three configurations without flaps.

The curves of C_M versus C_L for the complete airplane without flaps are shown in Figures 6, 7 and 8. Disregarding the changes in slope and intercept of the moment coefficient curves in the region below a lift coefficient of 1.0, which will be taken up as an effect on wing alone and tail moment coefficients, the predominant feature of these curves is the appearance of a large unstable hump with power on, near the stall, when the stabilizer is in the bottom position. In the upper middle position this hump is greatly reduced. In the top position it has completely disappeared. The elimination of this unstable hump near the stall, from the "power on" stability curves, as a result of locating the horizontal surfaces in a higher position relative to the wings and thrust line, is believed to be one of the most important results of this investigation.

Curves of the moment coefficient of wing and fuselage alone are also plotted on these figures, so that complete analysis is easily possible for each configuration. Curves of C_M versus C_L for the two flap arrangements are given in Figures 9 and 10. The unstable hump also appears in these curves, the horizontal stabilizer being in the bottom position.

(c) Component Parts of Moment Coefficient

Dr. C. B. Millikan has proposed in his course on the Aerodynamics of the Airplane that the static longitudinal stability of an airplane without power may be expressed in the form:

$$C_M = C_{M_W} + C_{M_F} + C_{M_t}, \text{ where}$$

$$C_{M_W} = C_{M_o} + \left(\frac{d}{t} - \frac{h}{t}\right)C_L$$

$$C_{M_F} = \Delta C_{M_o} + \Delta F C_L$$

$$C_{M_t} = -\eta_t \frac{\ell}{t} \frac{S_t}{S} \left[\frac{1 - \frac{a_o}{\pi AR}}{1 + \frac{a_o}{\pi AR_t}} C_L - \frac{a_o}{1 + \frac{a_o}{\pi AR_t}} \alpha_d \right]$$

In writing this equation certain simplifying assumptions have been made, as follows:

a) The wing is assumed to have an elliptical lift distribution.

b) The downwash at the tail is assumed to be twice the downwash at the wing.

c) A tail efficiency factor η_t is introduced to account for the effective velocity at the tail and to correct for other errors due to the simplifying assumptions used. The value of η_t can easily be determined graphically by taking the slope of the C_{M_t} versus C_L curve at the C_L range desired. Then differentiating the tail moment expression with respect to C_L we get:

$$\frac{dC_{M_t}}{dC_L} = -\eta_t \frac{\ell}{t} \frac{S_t}{S} \left[\frac{1 - \frac{a_o}{\pi AR}}{1 + \frac{a_o}{\pi AR_t}} \right]$$, where η_t is the only unknown quantity.

(d) Slipstream Effects on Wing and Fuselage

Considering the wing and fuselage without tail, it is interesting to investigate the effect of power on the lift of the wing as well as on the moment.

A curve of C_L versus α with no propeller and with power for level flight is given in Figure 15. A considerable increase in lift coefficient near the stall and a delay in the stall are apparent. A method of calculating the "power on" lift coefficient is given in "Theoretical Calculations". The calculated curve is also shown in figure 15 and as may be seen, the calculated curve gives a close approximation to the measured values.

The wing and fuselage moment coefficients were determined together both power off and power on.

$$C_{M_F} + C_{M_W} = C_{M_o} + \Delta C_{M_o} + (\frac{d}{t} - \frac{h}{t})C_L + \Delta F C_L$$

In Figure 11, C_{M_o} for a Clark Y section is plotted.

At $C_L = 0$, $C_{M_o} = -.065$

But at $C_L = 0$, $C_{M_F} + C_{M_W} = -.075$

Therefore $C_{M_o} = -.010$

$\frac{d}{t} - \frac{h}{t} = .30 - .25 = .050$ since center of gravity was assumed to be at .30t from leading edge.

As shown in Figure 11, $\Delta F = +.047$

$$C_{M_{W+F}} = C_{M_o} -.010 + (\frac{d}{t} - \frac{h}{t} + .047)C_L$$

Considering "power on" effects, write:

$$C_{M'_{W+F}} = C_{M_{th}} + C_{M_{W+F}} + \Delta C_{M'_o} + \frac{\Delta h}{t} C_L$$

Where $C_{M_{th}}$ = Moment Coefficient due to thrust =

$$\frac{T \times \text{Vertical Height of T above C.G.}}{qSt}$$

and $T = \frac{D}{\cos\alpha}$

$\Delta C_{M'_o}$ = change in C_{M_o} due to power

$\frac{\Delta h}{t}$ may be considered as a change in the location of the aerodynamic center due to power.

Values of $C_{M_{th}}$ were calculated at $C_L = 0$ and $C_L = 1.0$ and the increments not due to thrust, $\Delta C_{M'_o}$ and $\frac{\Delta h}{t}$ were obtained as follows:

a) $\Delta C_{M'_o}$ is the increment of wing-fuselage moment coefficient at $C_L = 0$ due to power except for that due to thrust.

Thus $\Delta C_{M'_o} = C_{M'_o} - C_{M_{th}(\text{at } C_L = 0)} - C_{M_{W+F}(\text{at } C_L = 0)}$

CORRECTION TO $C_{M_{NO\,TAIL}}$ FOR POWER

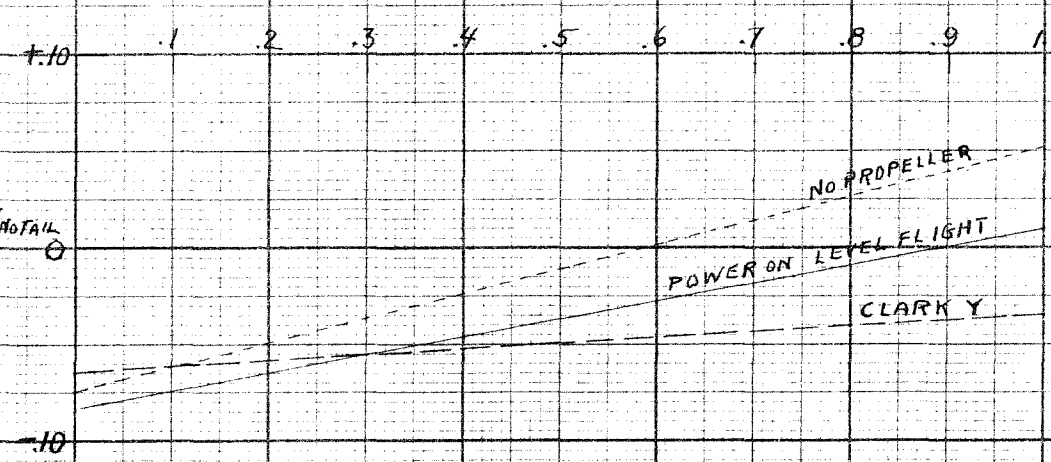

POWER OFF

$$C_{M_{NO\,TAIL}} = C_{M_W} + C_{M_F} = C_{M_o} + \Delta C_{M_o} + \left(\frac{d}{t} - \frac{h}{t}\right) C_L + \Delta F\, C_L$$

FROM ABOVE $\Delta C_{M_o} = -.010$

$$\Delta F = +.097 - \left(\frac{d}{t} - \frac{h}{t}\right) = +.097 - .050 = +.047$$

POWER ON

$$C_{M_{NO\,TAIL}} = C'_{M_W} + C'_{M_F} = C_{M_o} + \Delta C_{M_o} + \Delta C'_{M_o} + \left(\frac{d}{t} - \frac{h}{t} + \frac{\Delta h}{t}\right) C_L + \Delta F C_L + C_{M_{th}} = C_{M_{W+F}} + C_{M_{th}} + \Delta C'_{M_o} + \frac{\Delta h}{t}$$

VALUES OF $\Delta h/t$ AND $\Delta C'_{M_o}$ VARY WITH POWER. VALUES OBTAINED ARE PLOTTED BELOW.

$C_{M_{th}} = \frac{\text{MOMENT DUE TO THRUST}}{q\,S\,t}$, MUST BE INCLUDED IN CALCULATING $C'_{M_{W+F}}$ FOR ANOTHER AIRPLANE, USING $T = \frac{D}{\cos\alpha}$

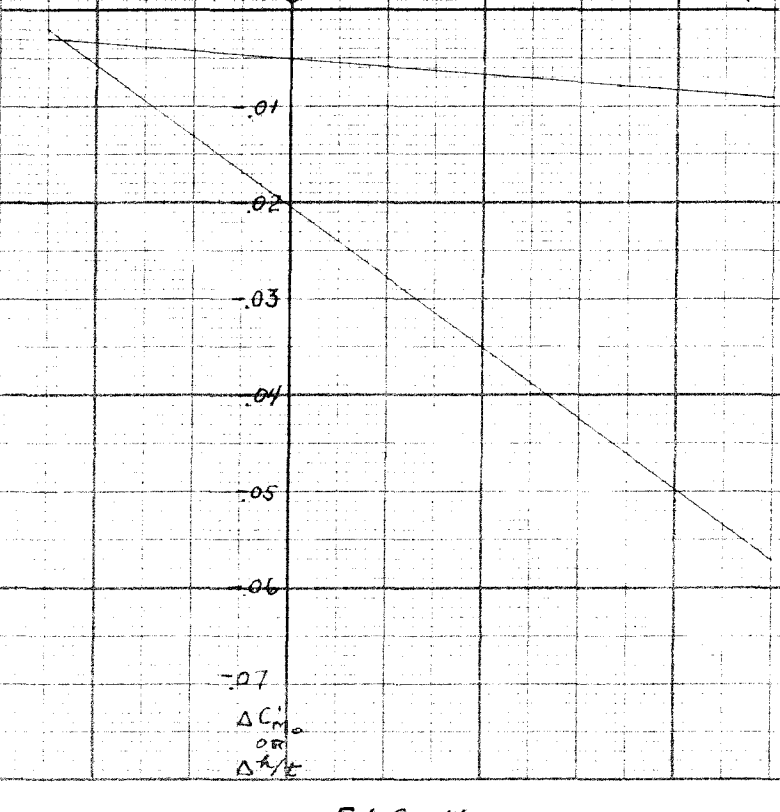

IN APPLYING $\Delta C'_{M_o}$ AND $\frac{\Delta h}{t}$ TO ANOTHER AIRPLANE CORRECT FOR PERCENT OF WING AREA IN SLIPSTREAM

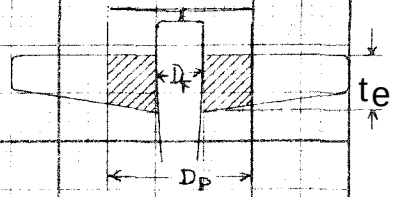

USE $S_e = (D_P - D_F) \times t_e$

FOR MODEL, $\frac{S_e}{S} = .127$, $\frac{1}{S_e/S} = 7.8$

$$\frac{\Delta h}{t}_{CORRECTED} = \frac{S_{e_2}/S_2}{S_{e_1}/S_1} = \frac{S_e}{S} \times 7.8 \times \frac{\Delta h}{t}$$

$$\Delta C'_{M_o\,CORRECTED} = \frac{S_e}{S} \times 7.8 \times \Delta C'_{M_o}$$

FIG. 11

b) $\frac{\Delta h}{t}$ is the change in slope of the wing fuselage moment coefficient curve due to power, except for that due to thrust.

$$\text{Thus } \frac{\Delta h}{t} = \frac{dC_{M'_{W+F}}}{dC_L} - \frac{dC_{M_{W+F}}}{dC_L} - \frac{dC_{M_{th}}}{dC_L}$$

Figure 11 gives the results obtained as a function of tan θ . A method of predicting $C_{M'_{W+F}}$ for other airplanes is also given.

A calculated curve of wing and fuselage moment coefficient, power on, versus angle of attack was also prepared. The method used and results obtained are discussed in "Theoretical Calculations".

(e) Slipstream Effects on Tail Moments

If the values of moment coefficient for wing and fuselage alone are subtracted from the values obtained for the complete airplane, the tail moment coefficients will be obtained.

Values thus obtained were plotted and straight lines drawn through the portions below a lift coefficient of 1.0. These faired curves of C_{M_t} versus C_L for the three stabilizer positions are shown in Figure 12.

The effect of power on stability consists of a change in the slope of the tail moment coefficient curve, dC_{M_t}/dC_L and a change in the intercept for any given deviation of the elevator from a neutral position.

For power off, write:

$$C_{M_t} = -\eta_t \frac{\ell}{t} \frac{S_t}{S} \left[\frac{1 - \frac{a_o}{\pi AR}}{1 + \frac{a_o}{\pi AR_t}} C_L - \frac{a_o}{1 + \frac{a_o}{\pi AR_t}} \alpha_d \right]$$

$$\frac{dC_{M_t}}{dC_L} = -\eta_t \frac{\ell}{t} \frac{S_t}{S} \left[\frac{1 - \frac{a_o}{\pi AR}}{1 + \frac{a_o}{\pi AR_t}} \right]$$

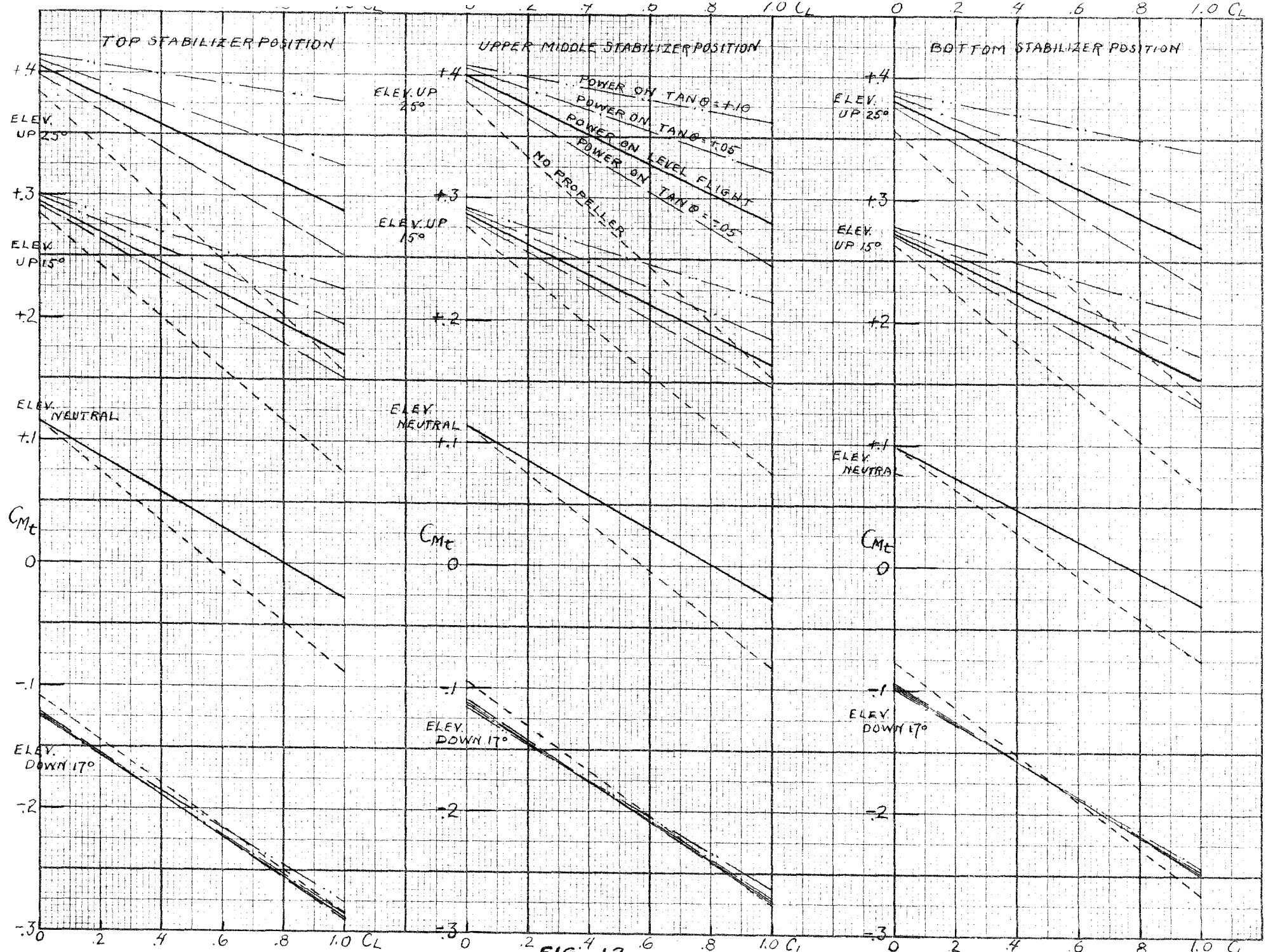
TOP STABILIZER POSITION
UPPER MIDDLE STABILIZER POSITION
BOTTOM STABILIZER POSITION
POWER ON TAN Θ = +.10
POWER ON TAN Θ = +.05
POWER ON LEVEL FLIGHT
POWER ON TAN Θ = -.05
NO PROPELLER
ELEV. UP 25°
ELEV. UP 15°
ELEV. NEUTRAL
ELEV. DOWN 17°
C_{M_t}
C_L
+.4
+.3
+.2
+.1
0
-.1
-.2
-.3
.2
.4
.6
.8
1.0

FIG. 12

If $\frac{dC_{M_t}'}{dC_L}$ = power on slope

Let $K = \dfrac{\frac{dC_{M_t}'}{dC_L}}{\frac{dC_{M_t}}{dC_L}}$

Similarly let:

$$\frac{\text{Change in moment due to elevator angle power on}}{\text{Change in moment due to elevator angle power off}} = \frac{\Delta C_{M_t}'}{\Delta C_{M_t}} = R$$

Then

$$C_{M_t}' = -\eta_t \frac{\ell}{t} \frac{S_t}{S} \left[K \frac{1 - \frac{a_o}{\pi AR}}{1 + \frac{a_o}{\pi AR_t}} C_L - R \frac{a_o}{1 + \frac{a_o}{\pi AR_t}} \alpha_d \right]$$

Values of K and R will vary with horizontal stabilizer location, elevator setting and amount of power.

In Figure 13, values of K and R have been plotted for each stabilizer location and for various amounts of power. The difference between the tail moment coefficient for a given elevator setting and the tail moment coefficient for neutral elevator, both at $C_L = 0$, is called ΔC_{M_t}. The values of K and R are plotted in Figure 13, against values of ΔC_{M_t} as abscissae. The elevator angles at which the changes in tail moment coefficient were measured are also indicated on this figure.

In Figure 14, values of K and R for various amounts of power and for different elevator angles have been plotted against vertical position of the horizontal stabilizer.

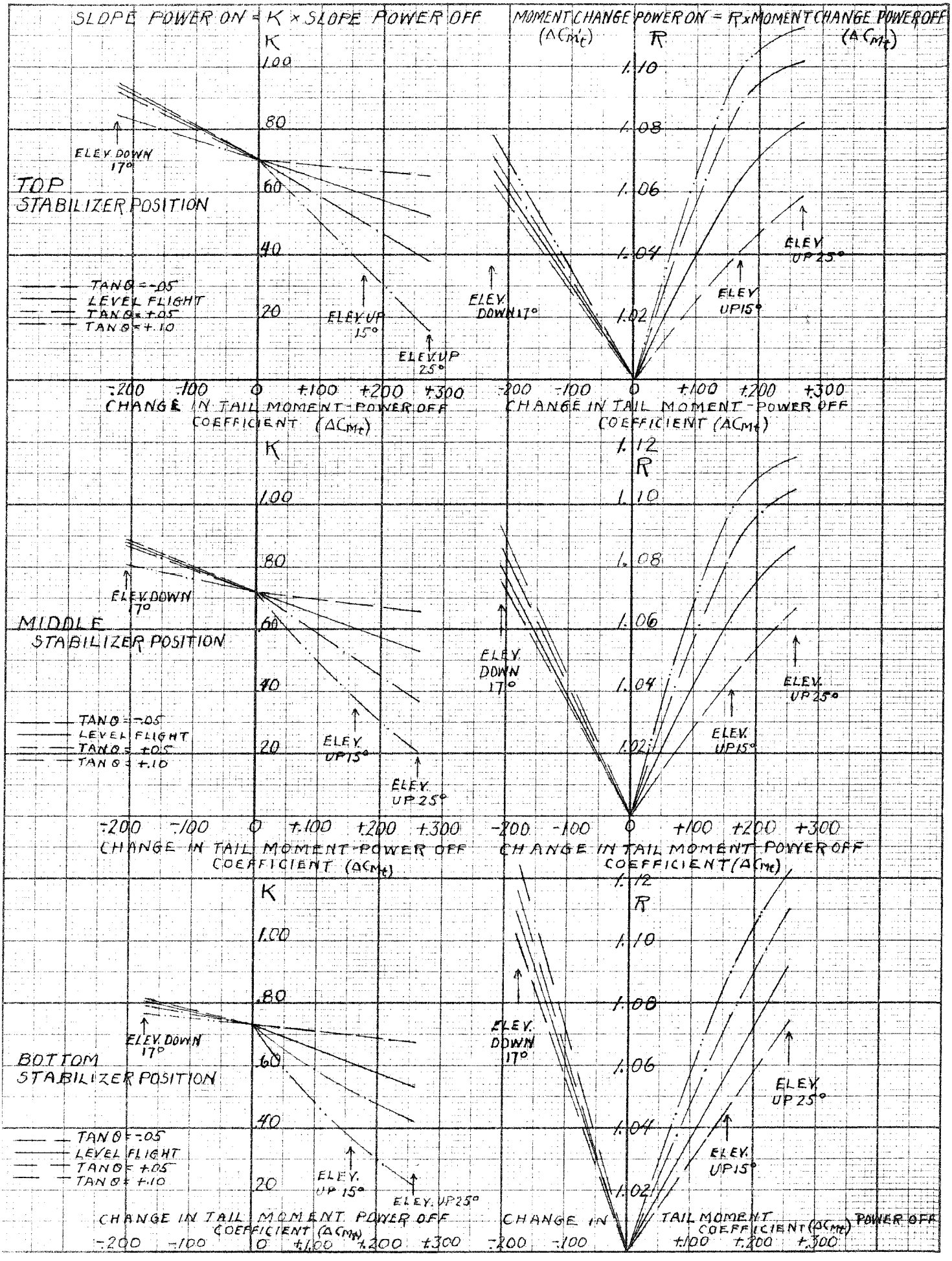
SLOPE POWER ON = K × SLOPE POWER OFF
MOMENT CHANGE POWER ON = R × MOMENT CHANGE POWER OFF
K
R
TOP STABILIZER POSITION
MIDDLE STABILIZER POSITION
BOTTOM STABILIZER POSITION
TAN θ = -.05
LEVEL FLIGHT
TAN θ = +.05
TAN θ = +.10
ELEV. DOWN 17°
ELEV. UP 15°
ELEV. UP 25°
CHANGE IN TAIL MOMENT - POWER OFF COEFFICIENT (ΔCMt)

FIG. 13

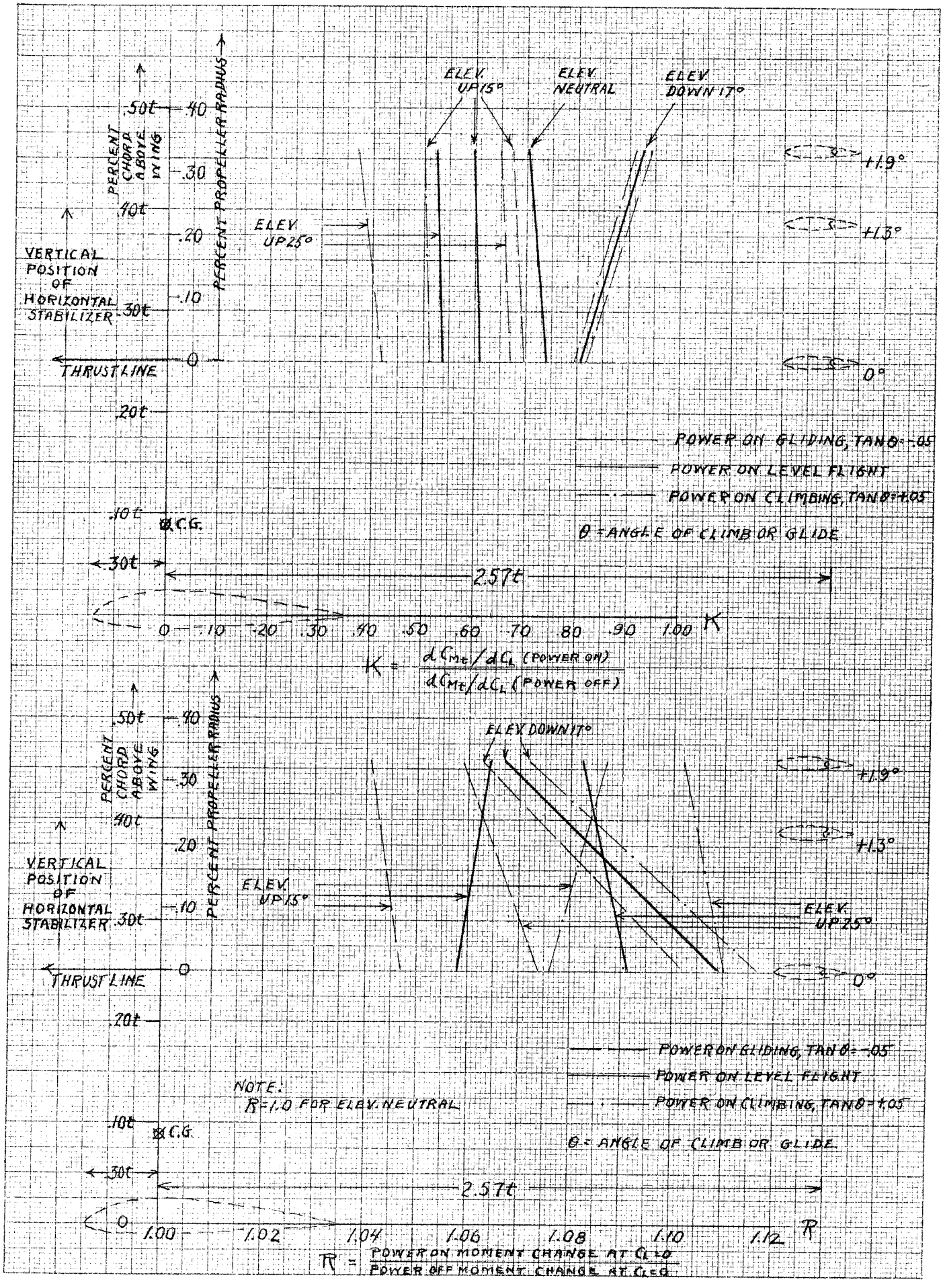
ELEV. UP 15°
ELEV. NEUTRAL
ELEV. DOWN 17°
ELEV. UP 25°
PERCENT CHORD ABOVE WING
PERCENT PROPELLER RADIUS
.50t
.40t
.30t
.20t
.10t
.30t
40
.30
.20
.10
0
VERTICAL POSITION OF HORIZONTAL STABILIZER
THRUST LINE
C.G.
.30t
2.57t
+1.9°
+1.3°
0°
POWER ON GLIDING, TAN θ = -.05
POWER ON LEVEL FLIGHT
POWER ON CLIMBING, TAN θ = +.05
θ = ANGLE OF CLIMB OR GLIDE
0
.10
.20
.30
.40
.50
.60
.70
.80
.90
1.00
K
$K = \frac{dC_{M_t}/dC_L \text{ (POWER ON)}}{dC_{M_t}/dC_L \text{ (POWER OFF)}}$
ELEV DOWN 17°
ELEV UP 15°
ELEV. UP 25°
NOTE:
R = 1.0 FOR ELEV. NEUTRAL
1.00
1.02
1.04
1.06
1.08
1.10
1.12
R
$R = \frac{\text{POWER ON MOMENT CHANGE AT } C_L = 0}{\text{POWER OFF MOMENT CHANGE AT } C_L = 0}$

FIG. 14

APPLICATION OF RESULTS TO WIND TUNNEL TESTS

The important change in configuration included in this investigation was the vertical position of the horizontal stabilizer. Figure 14, which gives values of K and R as a function of vertical height of horizontal stabilizer is considered the best presentation of results for application to wind tunnel tests on other low wing airplanes.

Assuming that the wind tunnel model of a proposed design has been tested with and without tail surfaces, curves of $C_{M\ \text{no tail}}$ versus C_L and C_{M_t} versus C_L, power off, should be available.

The "power on" curve of $C_{M\ \text{no tail}}'$ can be estimated as explained in Figure 11, or it can be calculated as suggested under "Theoretical Calculations".

In order to obtain C_{M_t}' versus C_L, enter Figure 14 with vertical height of stabilizer and pick off values K and R for desired power condition and elevator setting. These values must be corrected for difference in horizontal tail area exposed to the slipstream:

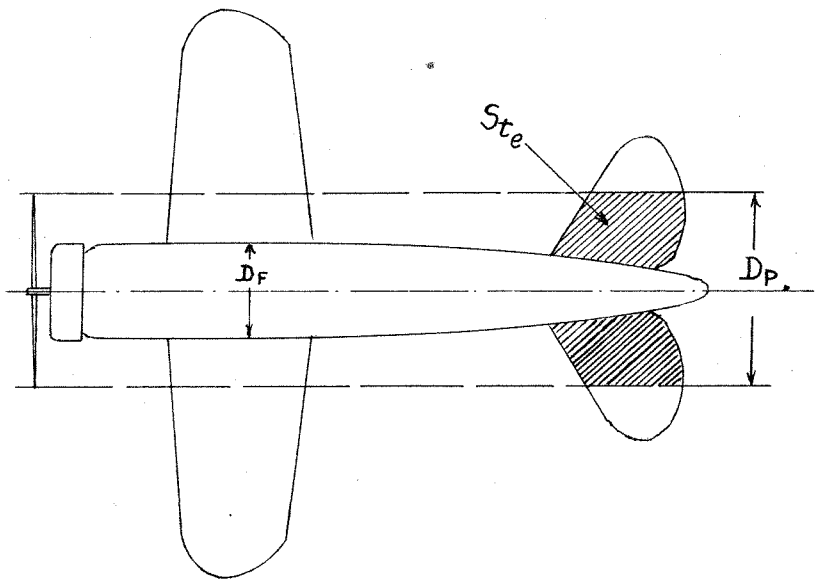

USE S_{te} = AREA INCLUDED BY LINES PARALLEL TO THRUST LINE AND A DISTANCE APART = D_P. D_P IS USED SINCE D_S IS APPROXIMATELY EQUAL TO D_P, CALCULATING D_S FROM: $\frac{\pi D_S^2}{4} = .8 \times \frac{\pi D_P^2}{4} + \frac{\pi D_F^2}{4}$

If S_{t_e} = horizontal tail area exposed to slipstream

S_t = horizontal tail area,

Corrected values of K and R can be calculated for application to other airplanes as follows:

$$K \text{ corrected} = 1 + \frac{S_{te}/S_t}{(S_{te}/S_t)_{MODEL}} (K-1)$$

$$R \text{ corrected} = 1 + \frac{S_{te}/S_t}{(S_{te}/S_t)_{MODEL}} (R-1)$$

But S_{te/S_e} of model = .67

$$K \text{ corrected} = 1 + \frac{S_{te}/S_t}{.67} (K-1)$$

$$R \text{ corrected} = 1 + \frac{S_{te}/S_t}{.67} (R-1)$$

THEORETICAL CALCULATIONS

It is interesting to investigate the possibility of estimating slipstream effects on the lift coefficient and moment coefficient of the wing based on purely theoretical considerations, and to compare the results thus obtained with experimental results.

(a) "Power On" Lift Coefficient

First considering the lift coefficient of the wing and fuselage:

LET PROPELLER DIAMETER = D_P

ASSUME THAT AT WINGS, WITH NO FUSELAGE PRESENT, SLIPSTREAM DIAMETER HAS CONTRACTED TO D_o, WHERE $\frac{\pi D_o^2}{4} = .8\ \frac{\pi D_P^2}{4}$

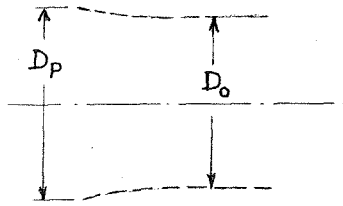

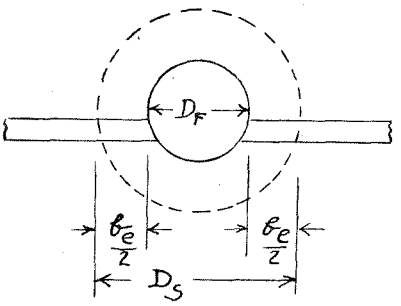

WITH FUSELAGE IN SLIPSTREAM, THE CROSS-SECTIONAL AREA OF SLIPSTREAM WILL REMAIN $\frac{\pi D_o^2}{4}$ BUT ITS ACTUAL DIAMETER D_S IS GREATER DUE TO PRESENCE OF FUSELAGE

$$\frac{\pi D_o^2}{4} = \frac{\pi D_P^2}{4} \times .8 \qquad \text{(correcting for contraction of slipstream)}$$

$$\frac{\pi D_o^2}{4} = \frac{\pi D_S^2}{4} - \frac{\pi D_F^2}{4}$$

$b_e = D_S - D_F$ = span in slipstream

$b_e \times t_e = S_e$ = area in slipstream

$$T = \frac{C_D q S}{\cos \alpha} \qquad C_T' = \frac{T}{q \times \frac{\pi D_o^2}{4}}$$

Referring to "Aircraft Propeller Design" by Weick, page 9, the propeller thrust coefficient C_T' can be written, $C_T' = 4a(1 + a)$ where 2a = increment of increase in slipstream velocity over flight velocity. This theoretically only holds far down stream. It has been assumed here that abreast the wing the slipstream has contracted to a cross-sectional area equal to eight-tenths the propeller disc area and that the slipstream velocity equals $V(1 + 2a)$.

$\Delta V_S = V \times 2a$ $\qquad$ $V_S = \sqrt{(V + \Delta V_S \cos\alpha)^2 + (\Delta V_S \sin\alpha)^2}$

$$\text{Tan } \Delta\alpha = \frac{\Delta V_S \sin\alpha}{V + \Delta V_S \cos\alpha}$$

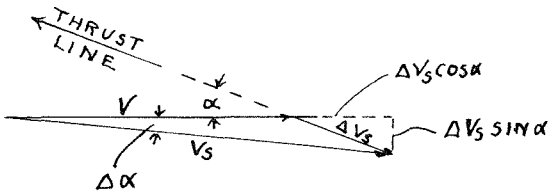

$$q_e = \frac{1}{2}\rho V_S^2$$

$$\Delta L_1 = q_e S_e C_{L_e}$$

where C_{L_e} = Lift coefficient at $\alpha - \Delta\alpha$

$$\Delta L_2 = T \sin\alpha$$

$$\Delta L_3 = (S - S_e) C_L q$$

$$C_L' = \frac{\Delta L_1 + \Delta L_2 + \Delta L_3}{S C_L q}$$

Values of C_L' versus α calculated in this manner are plotted, together with experimental values of C_L' in Figure 15.

(b) "Power On" Wing and Fuselage Moment Coefficient

$$C_L = \frac{\text{Lift}}{qS}$$

$$C_M = \frac{\text{Moment}}{qSt}$$

$$C_{M_e} = C_{M_o} + \left(\frac{d}{t} - \frac{h}{t}\right) C_{L_e}$$

It has been assumed here that the slipstream effects have not changed C_{M_o} and h/t. Actually some change has probably occurred.

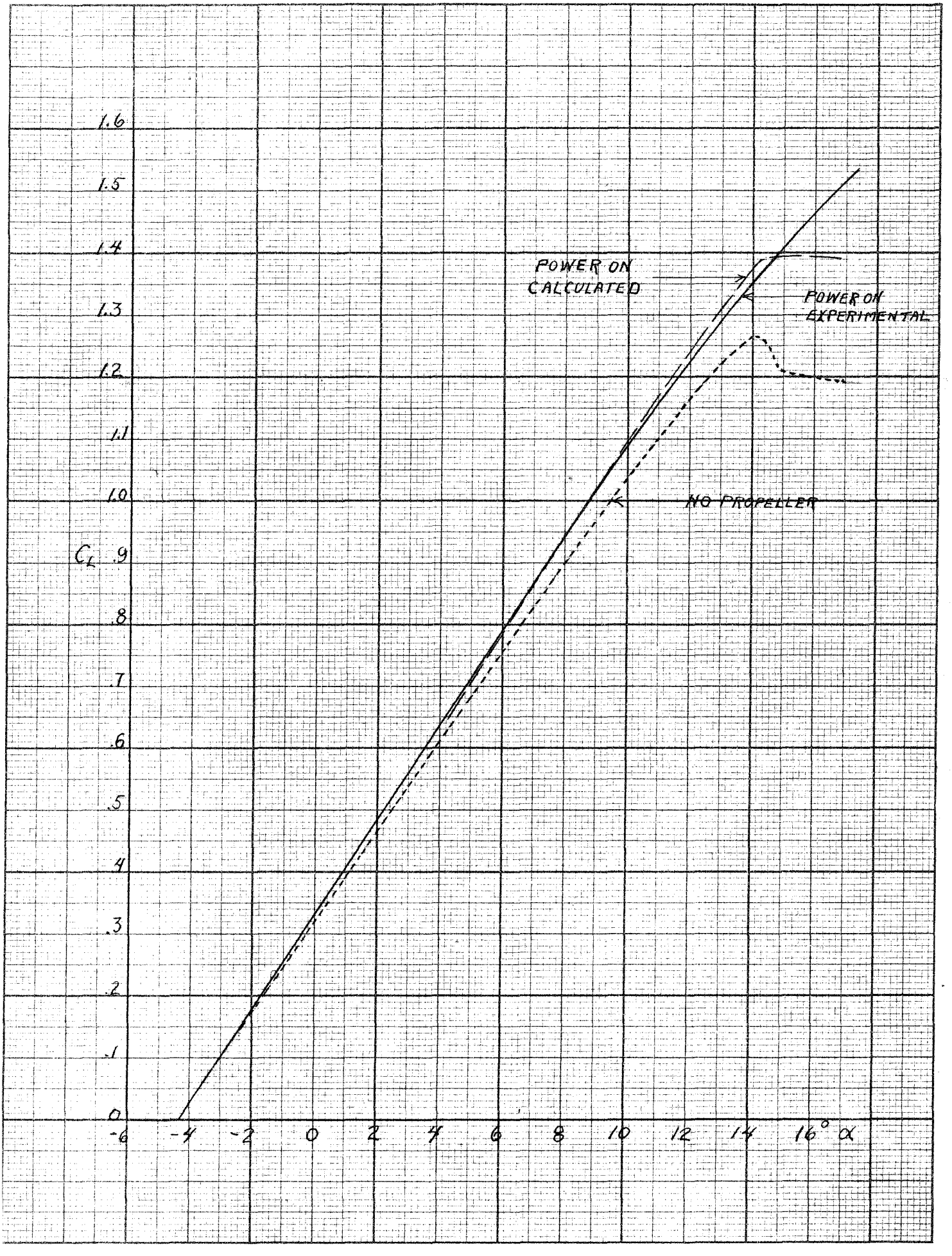
1.6
1.5
1.4
1.3
1.2
1.1
1.0
C_L .9
.8
.7
.6
.5
.4
.3
.2
.1
0
-6
-4
-2
0
2
4
6
8
10
12
14
16° α
POWER ON CALCULATED
POWER ON EXPERIMENTAL
NO PROPELLER

FIG. 15

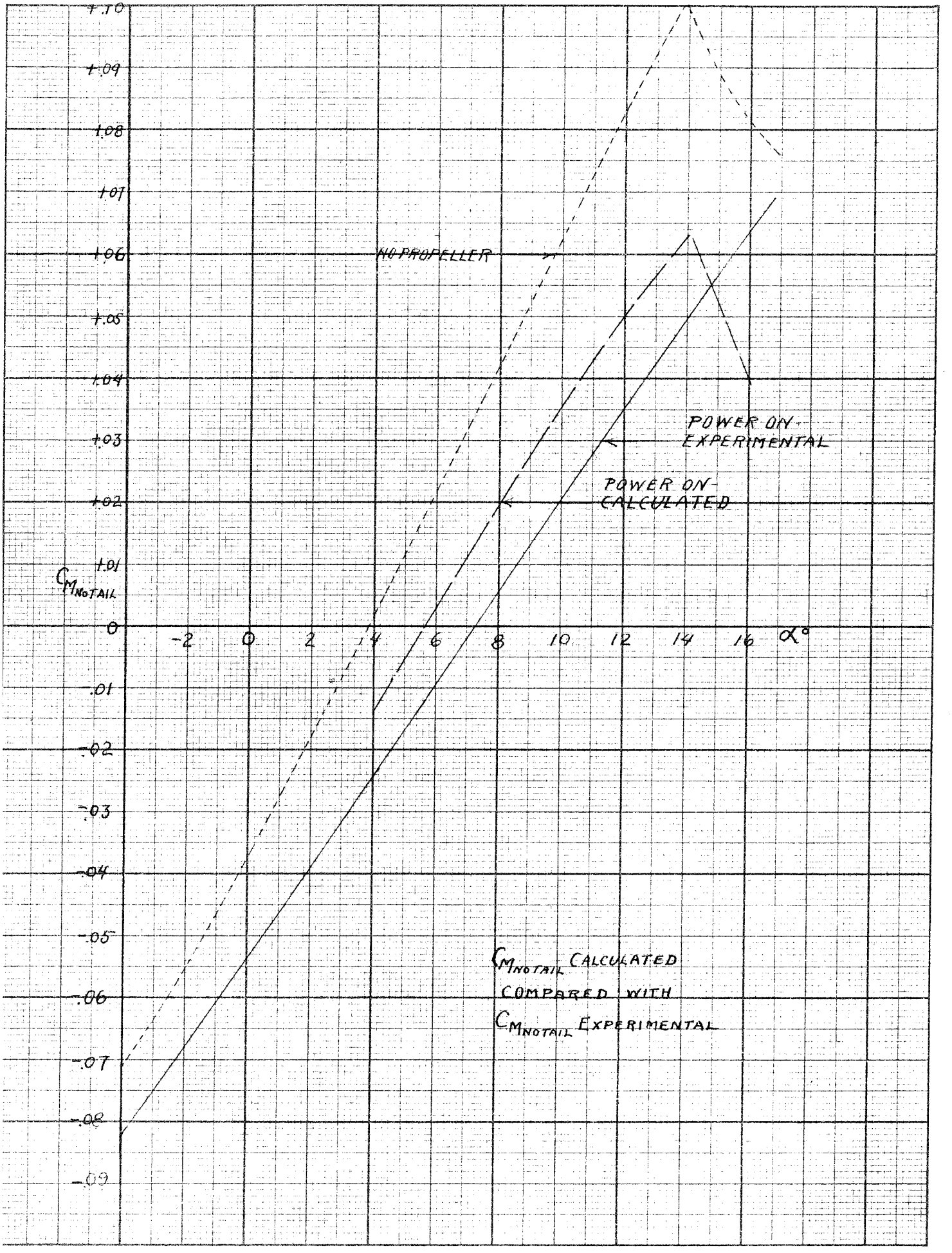
+.10
+.09
+.08
+.07
+.06
+.05
+.04
+.03
+.02
+.01
0
-.01
-.02
-.03
-.04
-.05
-.06
-.07
-.08
-.09
$C_{M_{NO\,TAIL}}$
NO PROPELLER
POWER ON-
EXPERIMENTAL
POWER ON-
CALCULATED
-2
0
2
4
6
8
10
12
14
16
α°
$C_{M_{NO\,TAIL}}$ CALCULATED
COMPARED WITH
$C_{M_{NO\,TAIL}}$ EXPERIMENTAL

FIG. 16

$$M_e = C_{M_e} q_e S_e t_e = \left[C_{M_o} - \left(\frac{d}{t} - \frac{h}{t}\right) C_{L_e} \right] q_e S_e t_e$$

$$\Delta C'_{M_1} = \frac{Me}{qSt}$$

$$\Delta C'_{M_2} = \frac{Mth}{qSt}$$

$$\Delta C'_{M_3} = \frac{Mr}{qSt} = \frac{C_M qt(S - Se)}{qSt}$$

$$C'_{M_{W+F}} = \Delta C'_{M_1} + C'_{M_2} + C'_{M_3}$$

Values of $C'_{M_{W+F}}$ have been calculated. Results obtained are plotted, together with experimental "power on" values, in Figure 16. Apparently the fuselage and fillet effects so alter the moment that this calculation gives only a poor approximation to actual "power on" moments. It is probable, however, that the discrepancy between calculated and experimental results would be about the same for similar configurations. Thus $C'_{M_{W+F}} - C_{M_{W+F}}$ if $C'_{M_{W+F}}$ is calculated, should be multiplied by about 1.7 to give values agreeing with experimental results.

CONCLUSIONS

1. Calculated values of C_L' agree closely with experimental "power on" results.

2. Calculated values of $C_{M_{W+F}}'$ do not agree with experimental values unless a multiplicative factor of 1.7 is applied.

3. Power improves the stability of the wing and fuselage alone and increases the increment of moment coefficient due to fuselage effects at $C_L = 0$.

4. Power decreases the slope of the tail moment coefficient curves as amount of power is increased. This decrease in slope expressed as a percentage does not change materially with vertical position of horizontal stabilizer in the region well below the stall.

5. Power increases the amount of moment caused by a movement of elevator from neutral to either an up or down position.

6. In the vicinity of the stall, power creates an unstable hump in the tail moment coefficient curves, when the stabilizer is on or near the thrust line. This hump disappears if the horizontal stabilizer is located relatively as high as the top position used in this investigation. Presumably higher positions would also be satisfactory.

7. With split flaps set at 45°, power decreases the stability in "power on" gliding flight. For a gliding angle such that $\tan \theta = -.10$, the decrease in stability is approximately the same as for the unflapped wing in level flight, when flaps are cut out under the fuselage. The decrease in stability with power for flaps continuous under the fuselage is more severe and stability for "power on" gliding flight at $\tan \theta = -.10$ with such flaps corresponds approximately to the stability of the unflapped airplane in climbing flight where $\tan \theta = + .05$.

ACKNOWLEDGMENT

Work with a power plant model of the type used for this investigation necessarily introduces many complications not encountered in ordinary wind tunnel tests. Grateful acknowledgment is made to the entire staff of wind tunnel assistants and to Lieutenant M. K. Fleming, U. S. N., for the cheerful assistance rendered, to Dr. C. B. Millikan for his many helpful suggestions and general supervision of this investigation, and to Dr. Theo. von Karman for his stimulating interest in the entire project.

SUPPLEMENTARY REPORT

ON

WIND TUNNEL TESTS OF THE EFFECT OF POWER ON THE STABILITY OF A LOW WING MONOPLANE WITH THREE VERTICAL POSITIONS OF HORIZONTAL TAIL SURFACES

AND

THREE BLADED PROPELLER CHARACTERISTICS AT BLADE ANGLES OF 32°, 36°, 40° AND 44°

by

Calvin M. Bolster

List of Illustrations and Charts

Introduction

During the winter of 1935-36, an investigation entitled "Wind Tunnel Tests on the Effect of Power on the Stability of a Low Wing Monoplane with Three Vertical Positions of Horizontal Tail Surfaces" was conducted and reported on. The present investigation is a continuation of the same problem and the stability portion of it consists of work which was omitted from the first series of tests due to lack of time.

The model used for these tests, dimensions of which are shown in Figure 1, was a 1/6th scale low wing monoplane with a Northrop "Alpha" wing and XTBD-1 tail surfaces. This is the same model as that used in the original investigation; however, for the present tests the torque measuring apparatus in the model was slightly modified in an effort to improve its accuracy. An improved operating technique was also developed.

Propeller characteristics are obtained in a wind tunnel by measuring the torque and r.p.m. of the propeller, simultaneously reading the net thrust of the propeller on the wind tunnel drag balance. These measurements are made at several different wind tunnel velocities with various amounts of power for each blade setting, in order that values of propulsive efficiency, advance ratio and speed-power coefficient can be computed for the complete range of these coefficients. For a detailed discussion of the method used in obtaining propeller characteristics with a wind tunnel model, see "Wind Tunnel Tests on a High Wing Monoplane with Running Propeller" by J. S. Russell and H. M. McCoy, reported in the Journal of Aeronautical Sciences dated January 1936.

The present propeller investigation was undertaken primarily for the purpose of improving the apparatus and the methods used in operating it, in an effort to obtain more accurate and dependable results. The blade angles tested were selected because the work previously done at the California Institute of Technology did not cover this range.

The notations used in this report for stability purposes are identical with those used in the basic paper. The propeller symbols are the standard ones as used by Weick in N.A.C.A. Report No. 350.

Description of Apparatus

The model used in this investigation was identical with that described in the original report. The important dimensions are shown in Figure 1. A slight change was made in the torque measuring apparatus in that the block which holds the coils used in this device was machined in one piece out of solid brass for this series of tests. The coils were each mounted on the block by four set screws and for the present investigation these set screws were tightened and then securely held in place by soldering a stiff wire to the heads of the screws. This alteration effectively prevented any slippage of the coils and improved the dependability of the apparatus.

Procedure

The results of the previous investigation into the effect of power on the stability of a low wing monoplane with different vertical locations of the horizontal stabilizer had shown that with no flaps a large unstable hump appeared in the moment coefficient curve near the stall, when the horizontal stabilizer was in the bottom position as

shown on Figure 1. This condition disappeared when the horizontal stabilizer was in the top position. Similar unstable portions occurred in the stability curves obtained for the flapped configurations which were tested, in the original investigation, only with the horizontal stabilizer in the bottom position. One purpose of this supplementary investigation was therefore to obtain curves of C_M versus C_L power on and power off with flaps with the horizontal stabilizer in the top position. Since no data had previously been taken with flaps but without tail surfaces, these runs were also made both with and without power. When plotted on the moment coefficient charts for the complete airplane, subtraction of the "no tail surface" data makes it possible to calculate the tail moment coefficients readily. The effect of power on the tail moment coefficient, with flaps on the airplane, can thus be easily obtained if desired.

The actual procedure for obtaining the power on and power off curves of C_M versus C_L was identical with that described in the original report. Also, as before, power is expressed in terms of the tangent of the angle of glide. For the stability tests, the propeller blades were set at an angle of 29 degrees at three-quarters radius.

The propeller characteristics were obtained with the propeller thrust axis horizontal. No flaps were installed and the horizontal stabilizer was in the top position for all the propeller tests. The chief source of error in previous propeller data had occurred in the torque measuring device. Calibrations indicated a definite change in torque reading due to changes in temperature of the model. In order to minimize these effects, the model was heated to 120 degrees F. before calibrating, and the propeller runs were made, starting in the high torque range for each wind tunnel "q", then gradually reducing the power input to the propeller. This procedure tended to heat the model rapidly

in the torque range where temperature effects were small, and once hot the model did not cool off rapidly as power was decreased. This operating technique gave improved consistency in the propeller data obtained.

In working up the propeller data, some scatter occurred when the values of propulsive efficiency "η" were calculated and plotted versus the speed power coefficient "C_s" direct from the observed data. However, values of the thrust coefficient $T_c = T/2qD^2$ and the torque coefficient $Q_c = Q/2qD^3$, when plotted against V/nD gave definite curves with small scatter. The method used in working up these data consisted of plotting T_c and Q_c against V/nD, fairing in a final curve for each, picking off values of T_c and Q_c from this curve for given values of V/nD and calculating η and C_s. These calculated valves of η versus C_s and V/nD versus C_s were plotted with the experimental points and final curves drawn in favoring the calculated values based on the T_c and Q_c curves. This method apparently gives consistent and reliable data.

Results

The curves of moment coefficient versus lift coefficient with power on and with no propeller were obtained in this investigation with flaps continuous under the fuselage and with the stabilizer in the top position. These results are shown in Figure 3. When compared to the curves given in Figure 3, which are for a similar configuration except that the horizontal stabilizer was in the bottom position, it may be seen that the unstable hump which occurred near the stall is considerably reduced with the horizontal stabilizer in the top position. With flaps the improvement is not as marked as without flaps; however, it is evident that the higher stabilizer position is desirable both with and without split flaps.

The curves of moment coefficient versus lift coefficient without tail surfaces are shown in Figures 2, 3 and 4. They are normal and need no comment.

The propeller characteristics for blade angles of 32°, 36°, 40° and 44° at 75 percent radius are shown in Figure 5. It will be noted that there is only a slight decrease in the peak propulsive efficiency at high blade angles.

The present tests were conducted using the three bladed propeller used by J. S. Russell and H. M. McCoy, except that ten percent of the blade length was cut off each blade at the tip. Their tests were carried out on a high wing monoplane, whereas the present data were obtained with a low wing monoplane. Comparing the curve of "η" versus "C_s" obtained for a blade angle of 32 degrees to that obtained previously as shown in Figure 6, it may be seen that cutting off the blades has reduced the peak efficiency about one and one-half percent and that the propulsive efficiency falls off more rapidly at high values of C_s. The "V/nD" versus "C_s" curve for β of 32 degrees lies above and to the left of that obtained on the previous test. This should be of interest in that it shows the general effect of cutting off the tips of propeller blades on a three bladed propeller.

Conclusions

(a) Stability Tests

With the horizontal stabilizer in the top position and with split flaps, power tends to decrease the stability in power-on gliding flight. The decrease in power on stability becomes much greater with increased values of up elevator angle. The unstable humps which occurred when the horizontal stabilizer was on the thrust line are considerably reduced if the horizontal stabilizer is mounted in the top position shown in Figure 1.

(b) Propeller Tests

Satisfactory propeller data can be obtained with the present GALCIT power model, the largest source of error now being due to temperature variation in the torque mechanism. Careful control of this temperature by proper operating procedure must be carried out in order to insure reliable results. Improvement lies in the direction of more accurate temperature control for the torque mechanism. The propeller data obtained are of interest in that they give the characteristics of a three bladed propeller mounted on a low wing monoplane with an N.A.C.A. cowling, at high propeller blade angles. They also show the general effect of cutting off the tips of propeller blades on the propeller characteristics and their mutual relations to each other.

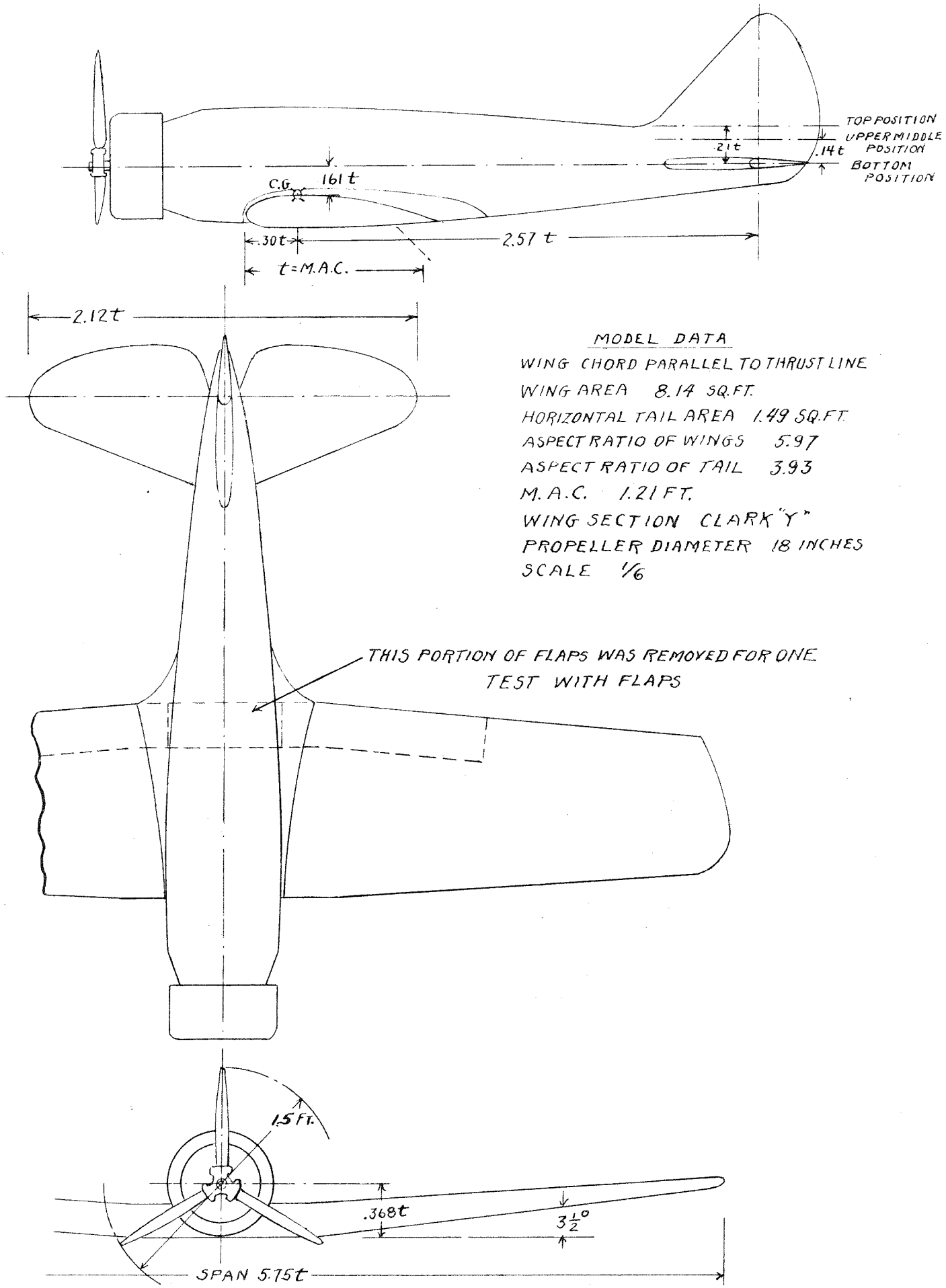

MODEL DATA

WING CHORD PARALLEL TO THRUST LINE
WING AREA 8.14 SQ.FT.
HORIZONTAL TAIL AREA 1.49 SQ.FT.
ASPECT RATIO OF WINGS 5.97
ASPECT RATIO OF TAIL 3.93
M.A.C. 1.21 FT.
WING SECTION CLARK "Y"
PROPELLER DIAMETER 18 INCHES
SCALE 1/6

FIG. 1

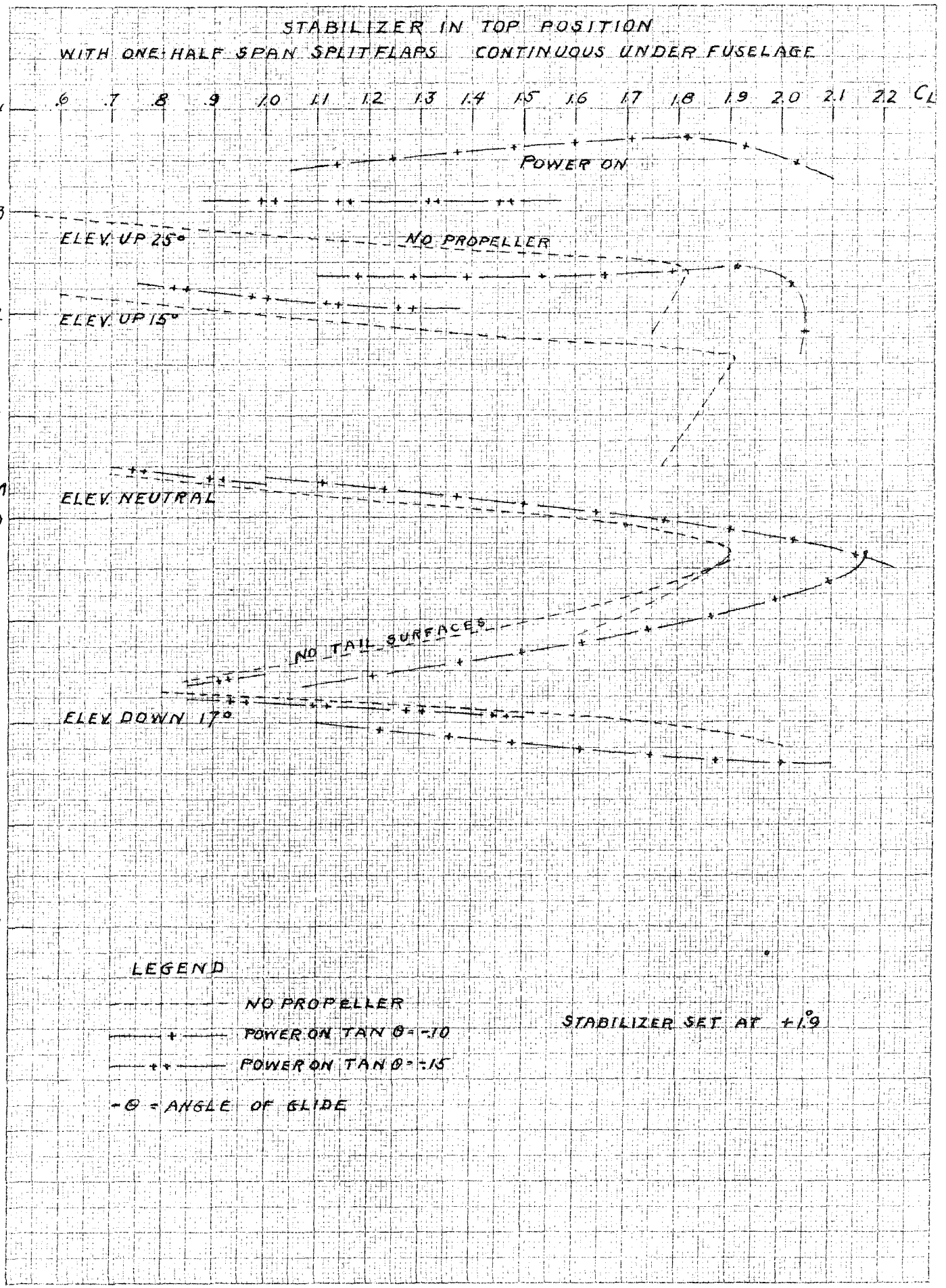
STABILIZER IN TOP POSITION
WITH ONE-HALF SPAN SPLIT FLAPS CONTINUOUS UNDER FUSELAGE
.6 .7 .8 .9 1.0 1.1 1.2 1.3 1.4 1.5 1.6 1.7 1.8 1.9 2.0 2.1 2.2 C_L
.4
.3
.2
.1
C_M
0
-.1
-.2
-.3
-.4
POWER ON
NO PROPELLER
ELEV. UP 25°
ELEV. UP 15°
ELEV. NEUTRAL
NO TAIL SURFACES
ELEV. DOWN 17°
LEGEND
NO PROPELLER
POWER ON TAN Θ = .10
POWER ON TAN Θ = .15
-Θ = ANGLE OF GLIDE
STABILIZER SET AT +1.9°

FIG. 2

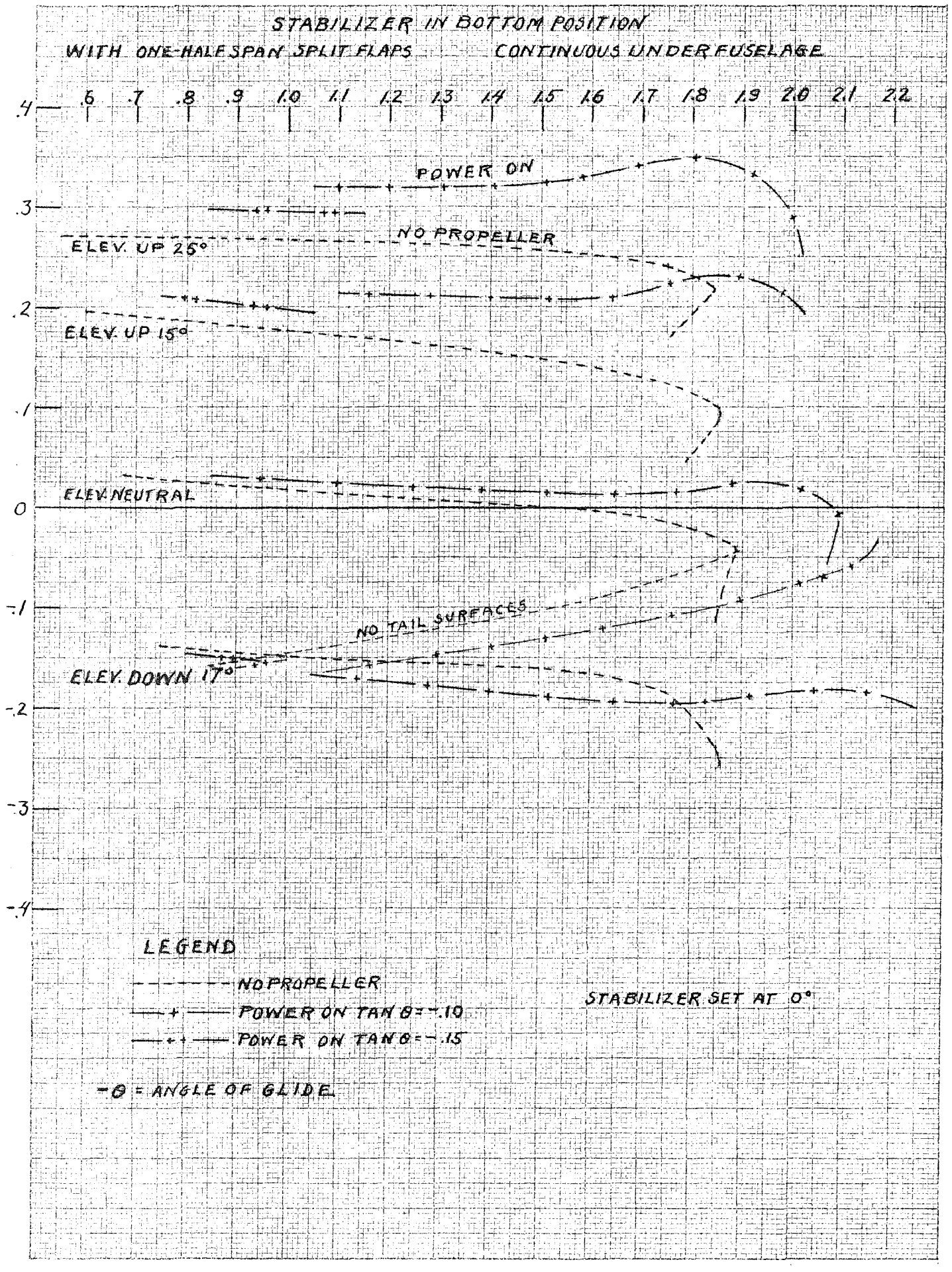
STABILIZER IN BOTTOM POSITION
WITH ONE-HALF SPAN SPLIT FLAPS CONTINUOUS UNDER FUSELAGE
.6 .7 .8 .9 1.0 1.1 1.2 1.3 1.4 1.5 1.6 1.7 1.8 1.9 2.0 2.1 2.2
.4
.3
.2
.1
0
-.1
-.2
-.3
-.4
POWER ON
NO PROPELLER
ELEV. UP 25°
ELEV. UP 15°
ELEV. NEUTRAL
NO TAIL SURFACES
ELEV. DOWN 17°
LEGEND
NO PROPELLER
POWER ON TAN θ = -.10
POWER ON TAN θ = -.15
STABILIZER SET AT 0°
-θ = ANGLE OF GLIDE

FIG. 3

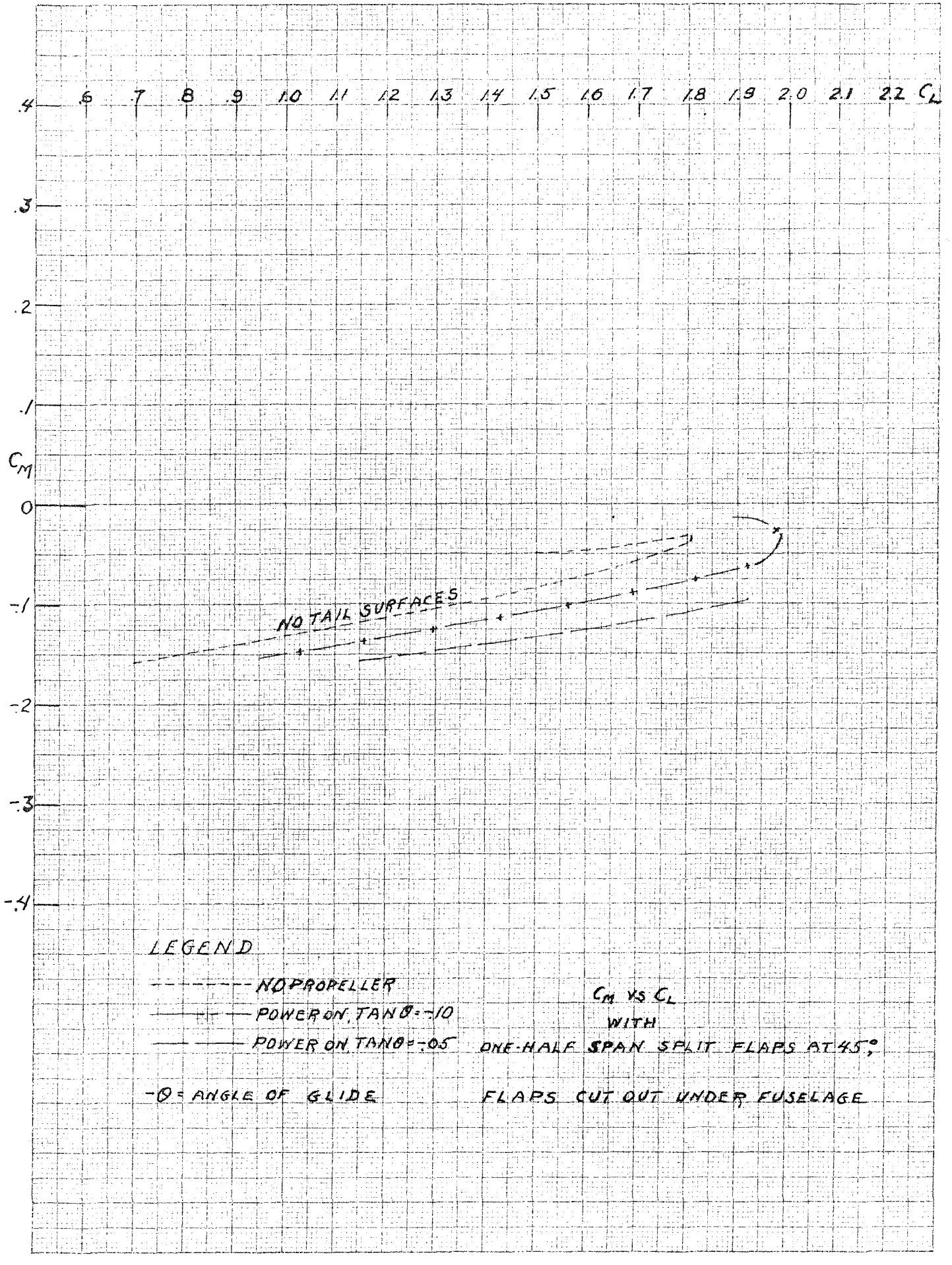
.6 .7 .8 .9 1.0 1.1 1.2 1.3 1.4 1.5 1.6 1.7 1.8 1.9 2.0 2.1 2.2 C_L
.4
.3
.2
.1
C_M
0
-.1
-.2
-.3
-.4
NO TAIL SURFACES
LEGEND
NO PROPELLER
POWER ON, TAN Θ = -.10
POWER ON TAN Θ = -.05
-Θ = ANGLE OF GLIDE
C_M VS C_L
WITH
ONE-HALF SPAN SPLIT FLAPS AT 45°
FLAPS CUT OUT UNDER FUSELAGE

FIG. 4

η

.90
.80
.70
.60
.50
.40
.30
.20
.10
.00

$\beta = 32°$ $36°$ $40°$ $44°$

$\beta = 32°$ $36°$ $40°$ $44°$

44°
40°
36°
$\beta = 32°$ AT .75 RADIUS

LINE OF MAX. η FOR C_S

2.5
2.0
1.5
1.0
.5
0

$\frac{V}{ND}$

0 .5 1.0 1.5 2.0 2.5 3.0 3.5 4.0

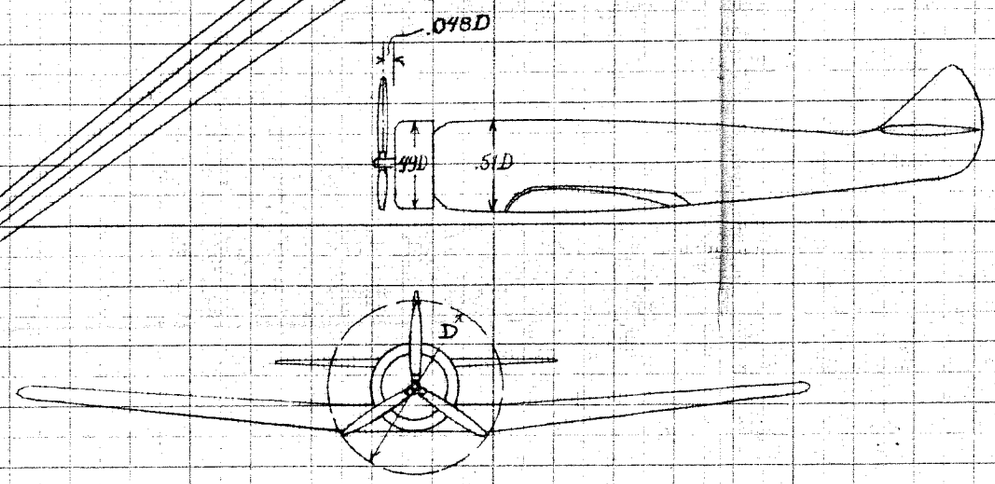

THREE BLADED PROPELLER CHARACTERISTICS

AT BLADE ANGLES ABOVE 32°

PROPULSIVE EFFICIENCY AND ADVANCE RATIO VS

SPEED-POWER COEFFICIENT FOR BLADE ANGLES

OF 32°, 36°, 40° AND 44°

FROM 1/6 SCALE MODEL TEST, USING HAMILTON-STANDARD

1A1-0 BLADE FORM WITH 10 PERCENT OF TIP CUT OFF.

CALIF. INST. OF TECH. SEPTEMBER 1936 LT-COMDR C.M. BOLSTER U.S.N.

FIG. 5 $C_S = \frac{\rho^{1/5} V}{N^{2/5} P^{1/5}}$

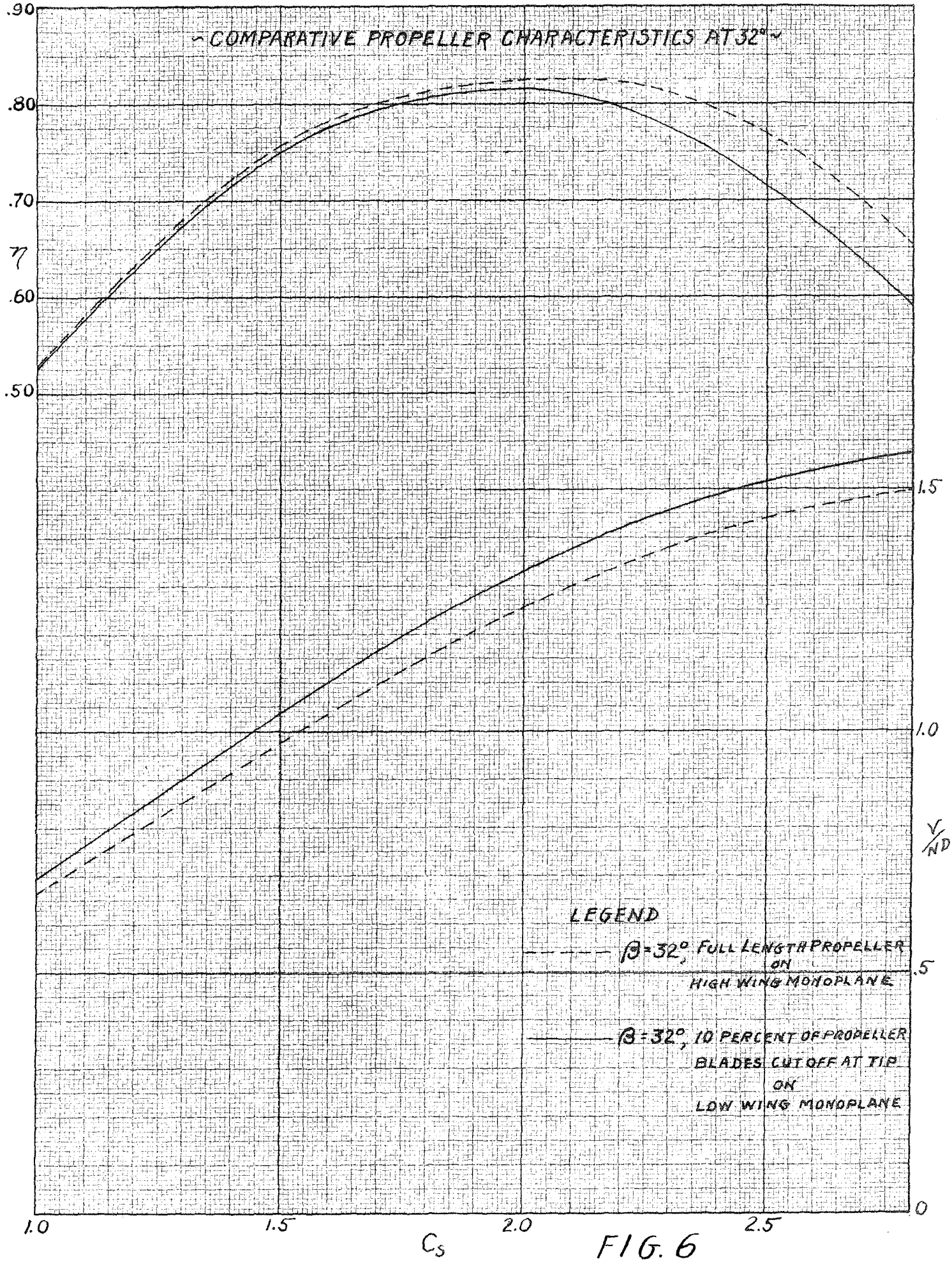
~ COMPARATIVE PROPELLER CHARACTERISTICS AT 32° ~
.90
.80
.70
.60
.50
η
1.5
1.0
.5
0
V/ND
LEGEND
β=32°, FULL LENGTH PROPELLER ON HIGH WING MONOPLANE
β=32°, 10 PERCENT OF PROPELLER BLADES CUT OFF AT TIP ON LOW WING MONOPLANE
1.0
1.5
2.0
2.5
Cs

FIG. 6